

## **4. Design of Al and Al-Li Alloys for Thixoforming**

*Bernd Friedrich, Alexander Arnold, Roger Sauermann, and Tony Noll*

### **4.1 Production of Raw Material for Thixoforming Processes**

A summary of the most important process alternatives for the forming of partially liquid metals is shown in Fig. 4.1. In the left-hand column, "conventional" thixoforming - which is currently most widely used for industrial applications – is schematically represented and in the right-hand column, the so-called "slug on demand" process.

The stress induced and melt activated (SIMA) process required conventional continuous-cast or extruded billets as feed material. Cold deformation of the billets induces high residual plastic strain. On reheating, recrystallization leads to a fine globulitic granular structure. The SIMA material exhibits very good properties, although it is only economical for special applications due to its high cost [2]. Mechanical agitation is one of the principle processes for the production of raw materials [3], but was never really successful. It was not possible to counter the corrosion and erosion of the agitating mechanism within the system [1], and on the process side the continuous casting procedure could not be synchronized with the agitation process.

The magnetohydrodynamic (MHD) process is to date the most widely used industrial process for production of raw material [1]. Grain refinement is achieved by motion of the bath induced by a magnetic field. This involves installing a solenoid coil on the permanent mould, fed with an alternating current. This measure can also be used to keep the permanent mould temperature homogenous at a desired value. In the semi-solid processing (SSP) process, just as in the MHD process, magnetic agitation is used to achieve grain refinement. The difference is that each billet is individually produced in its own chamber [4]. This offers the advantage of flexible alloy adjustment. Furthermore, the hot billets can be reprocessed straight from the chamber, so that advantages can be achieved from the viewpoint of energy considerations. On the other hand there are economical advantages in the alternative of semi-finished production.

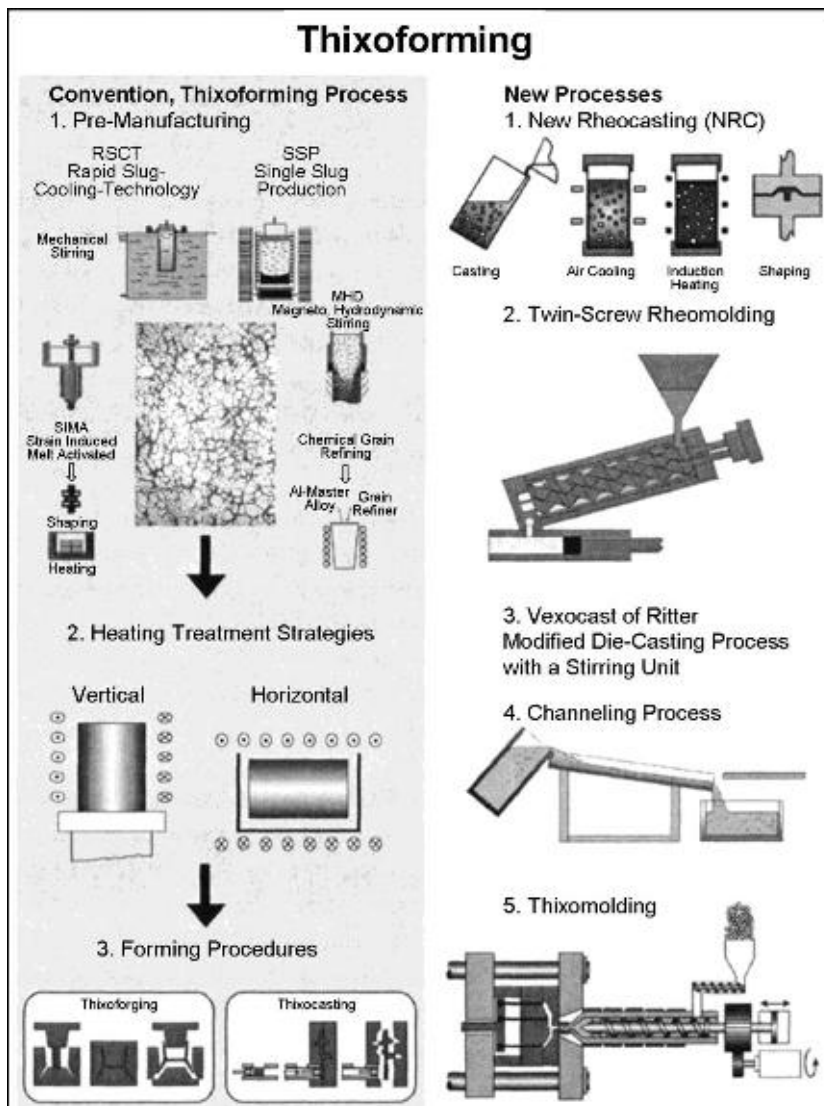


Fig. 4.1: Alternative thixoforming processes [1].

Chemical grain refinement is a process that offers lower processing costs and is from an economical point of view considered as an alternative to the other processes mentioned above [5]. The fine grain structure is achieved with the aid of alloying elements (e. g. AlTi5B1) that act as heterogeneous nucleating agents [5]. The grain refiners are in the form of a wire injected directly into the melt. Other elements can also be added to enhance the grain refining properties of these elements (so-called modification) [4]. It was furthermore verified that the chemical grain refinement of aluminium alloys has an advantageous effect on the "castability" and other technologically important properties. The further targeted development of an A356-AlSi7Mg0,3 alloy by means of grain refinement and modification using Ti and Sr was investigated in 2003 [6]. One possibility for further refinement of the grain structure is the combination of chemical refinement with the MHD process [7].

The raw material has to be reheated precisely to a target temperature in the solidus-liquidus range [8]. Rapid heating prevents undesired grain growth and makes higher cycling rates possible. In this respect, inductive heating offers advantages over other heating processes due to its inherent controllability and its frequency-dependent, relatively high penetration depth. During reheating the eutectic phase melts first. The liquid portion rises steeply with minimal heating at temperatures above 560°C. From ~570°C the entire eutectic phase is molten. At temperatures above 570°C the aluminium dendrites begin to melt. The liquid portion rises only slowly in this temperature range. The working temperature for reheating is precisely within the transformation range between fully molten eutectics and commencement of dendrite melting. Alongside its low temperature-sensitivity to the phase relationship, A356 has the characteristic that, in its partially liquid state, ~50 % primary phase and 50 % eutectic exist. Due to this composition there are material-specific advantages in terms of processing. Materials for which it is not possible to adjust the solid/liquid mixture so accurately require considerably more processing costs [7].

In the "slug on demand" or rheocasting processes the production of a suitable thixo-formed raw material is done straight from the fluid melt with direct forming of the partially liquid metal [1]. Various new rheocasting processes are briefly explained in the following (see Figure 4.1, right-hand column).

In new rheocasting (NRC), the melt is in a controlled manner cast into a crucible and thus cooled down to the desired temperature between solidus and liquidus states. This creates a fine-grained, globulitic solid phase. After a short homogenising phase the partially solidified material is fed directly on to the forging or casting process. In twin-screw rheomoulding the melt is fed into the machine via a casting gate. There are two interacting screw feeders, with a special profile to achieve high shear rates, to convey the material axially into the machine and where it is simultaneously cooled down to the partially liquid state. The high shear rate creates a fine-grained, globulitic grain structure. The partially liquid metal is dosed and pressed out of an opening into the filling chamber for forming in a modified die-casting machine. To date this process was only used for modelling alloys of the types PbSn15 and MgZn30. One difficulty with this process is the choice of a suitable material for the screw feeders, in order to avoid adherence of the metal and to minimise wear [1].

The Vexocast process was developed by the company Ritter in Germany [1]. The metallic suspension is produced directly out of the melt in a separate treatment chamber which is in combination with a holding furnace as with the casting

chamber. The melt is inductively agitated in the treatment chamber and in the freezing range a small quantity of metal powder is added to cool it down. One essential feature of the process is its short time range of only ~15 seconds for production of the metallic suspension. The channelling process represents a further application method of the "slug on demand" process. The two essential constituents of the trial setup for the channelling process are the casting channel and the forming basin. The channel has to provide for rapid cooling of the melt, down to a temperature below the liquidus temperature. This creates a very high number of active nuclei suspended in the melt. The melt flows from there into a ceramic forming basin installed directly underneath the channel. On cooling down in the partially liquid range, the high nucleus density created results in the formation of a globulitic primary phase.

The thixomoulding process entails injection die casting of partially liquid light metal alloys, predominantly Mg alloys [9, 10]. The original material, in the form of granulate or turnings, is transferred by powerful shear movements in a heated steel screw feeder, into a liquid metallic suspension. Subsequently the screw feeder performs a pushing motion to inject the material into the actual forming tool [11]. The proportion of solid material can be up to 65 % [12].

#### **4.2 Chemical Grain Refinement of Commercial Thixoalloys**

If a metal alloy has to be processed in a partially liquid state, it must conform to many requirements. The following criteria are among the most important:

- In the semi-solid range the alloy constitutes a globulitic solid phase with grain sizes of < 100  $\mu\text{m}$ .
- Within the semi-solid range the alloy exhibits low temperature-sensitivity of the liquid phase portion.
- The solid phase skeleton fractures down under shear load transferring the metallic suspension to low viscosity in the range of 1 Pas.

Furthermore, it is important that there is minimal grain growth in the material during the holding period in the partially liquid state, because the refinement of the solid phase ( $\alpha$ -aluminium) has a positive effect on its viscosity, the tendency to separation of the mixture and the achievable component wall thicknesses. A summary overview of the relevant requirements in relation to grain structure morphology, rheology and thermo-chemistry is given in Table 4.1. Many of these criteria are best met by the casting alloys already used on an industrial scale, such as A356 or AlSi7Mg0.3 - which explains their wide use in the thixoforming process. The most important non-technical requirements for thixoforming

materials are low material costs, which has to be realised in terms of raw material prices, simple production procedures, minimum number of processing operations and minimum wastage of residual materials. The choice of a suitable material inevitably determines all further processing operations. Systematic development of raw materials for thixoforming with the aid of alloying elements and grain refiners has been carried out to only a limited extent to date [6, 13].

Table 4.1: Essential requirements for thixoforming materials.

requirement (determination method)	Parameter	formula	target value
small grain size (metallography)	mean grain diameter	$d_m = f(\dot{T}, c)$	$d_m < 100\mu\text{m}$
globulitic structure (metallography)	form factor	$f = \frac{4 \cdot \pi \cdot A}{U^2}$	$f > 0.6$
small cross-linking of the dendrites (metallography)	contiguity	$C^{fs} = f^s \cdot \frac{2 \cdot S^{ss}}{2 \cdot S^{ss} + S^{sl}}$	$0.4 < C^{fs} < 0.6$
small cross-linking volume of the dendrites (metallography)	contiguity volume	$Vc = VsCs$	$0.1 < Vc < 0.3$
low viscosity of the melt under shear load (rheometer tests)	viscosity under shear load	$\eta = k \cdot \dot{\gamma}^{n-1}$	$\eta \sim 1 \text{ bis } 10 \text{ cP}$
defined solid/liquid phase ratio (DTA, simulation, metallography)	$F_{liq}$	$f_s = 1 - \left( \frac{T_M - T_L}{T_M - T} \right)^{\frac{1}{1-p}}$	40 - 60 mass. %
large melting interval (DTA, simulation)	$dT = (T_{liq} - T_{sol})$	$dT = f(c, \dot{T}, p)$	max. 130°K min. 70°K
temperature sensitivity (DTA, simulation)	stop at 50 % liquid portion	$df_l/dT$	$< 0.015$
temperature sensitivity	temperature sensitivity	$Df_s = 0.01 \cdot (df_s/dT) \cdot T_{ss}$	$\leq 0.06$
temperature sensitivity (DTA)	temperature sensitivity	$dT_{40-60}$	$> 10^\circ\text{K}$

with  $\eta$ : viscosity,  $k$ : constant,  $\dot{\gamma}$ : shear velocity,  $n$ : Oswald-de Waele exponent;  $d_m$ : mean grain diameter,  $f$ : forming factor,  $A$ : grain surface area,  $U$ : circumference of a grain,  $S^{ss}$ : the grain boundary surface area between the solid phase, i.e. the surface area between the cohering grains not separated melt,  $S^{sl}$ : phase boundary surface area between solid phase and melt,  $dT$ : melt range,  $f(c, \dot{T}, p)$ : function of (alloying element content, rate of cooling, pressure),  $f_s$ : proportion of solid material,  $T_M$ : melt temperature of a component;  $T_L$ : liquidus temperature;  $p$ : exponent defined by the phase state equilibria

#### 4.2.1 Methodology for Tuning of Commercial Alloys for Semi-solid Processing by Means of Grain Refinement

Because of its range of applications in the automotive, machinery and aerospace industries, as well as in shipbuilding and electrical engineering, the material A356 (EN AC-AISi7Mg0.3) is by volume one of the most important aluminium casting materials. This is primarily due to its low density and good mechanical properties,

such as high strength and toughness as well as its high corrosion resistance and suitability for welding and heat treatment. Due to these material characteristics the alloy has a good potential for light-weight construction. Furthermore the material is the most important raw material for the production of components by thixoforming. The solidification range of  $\sim 60^{\circ}\text{C}$  is within a range making it readily workable in its partially liquid state. The material reacts particularly well in the range of temperature-sensitivity of the phase portion as long as the liquid phase proportion is set  $> 50\%$ . On the basis of this material characteristic profile, the alloy A356 (EN AC-AISI7Mg0.3) is our choice for in-house working and has to be prepared to meet the requirements making it workable in its partially liquid state. This objective should in the first instance be followed up independent of any other processing route. Process technology for raw material production is primarily focussed on the input of a fine-grained basis grain structure. A series of different technical solutions are available for this purpose. The necessary fine grain structure should hence be created by the addition of a chemical grain refinement agent in combination with modification of the eutectic grain structure. Besides that the interaction of the employed chemical grain refiners with the modifying agents and other alloying elements is to be studied (Figure 4.2).

Additionally, the adaptation of the alloys has to be managed such that during reheating in the partially liquid state, grain growth is minimized [14].

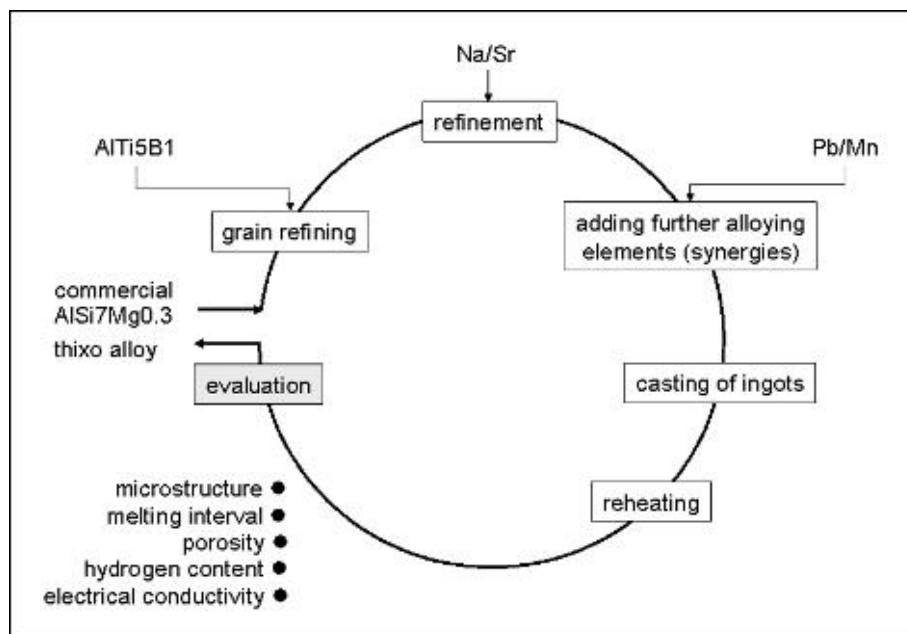


Figure 4.2: Procedure for adaptation of the alloy composition A356 (EN AC-AISI7Mg0.3) to the requirements of thixoforming.

#### 4.2.2 Adaptation of the Chemical Composition

The objective of this task is to identify the effect and the interaction of the standard chemical grain refiner AlTi5B1 with both the recognised modifying agents, sodium and strontium, as well as other elements (manganese and lead). To date there is little known about the mechanisms involved in the interactive effect between grain refinement and modifying agents. Within the framework of the melt testing, using the model-supported testing plan, various chemical compositions were produced and then evaluated in respect of the effect variables important for thixoforming. Particular attention was given to the grain size in the primary phase, modification of the eutectic phase, the melt range and the rheological characteristics.

For these parameters a mathematically linear approach was chosen for determination of the efficiency. For the parameters of titanium concentration and reheating time, the focus is on the question of how the parameters can be set in order to achieve optimum results for the effect variables. The standard grain refiner AlTi5B1 was used for chemical grain refinement. Lead was selected to test its possible positive effect on grain refinement. In minimal concentrations Pb already reduces the surface tension of aluminium and should therefore have a positive effect on grain refinement and/or modification. For strontium and sodium, 200 ppm was defined as the upper step value, in order to ensure its efficiency but at the same time to avoid over-modification. For the reheating time, periods of between 5 and 15 minutes are technically relevant. Particularly long holding times may however be unavoidable in the event of process malfunctions during reheating, so the suitability of the raw material was also tested in this respect.

The titanium content and the reheating time can be identified as significant influences on the grain size. As the titanium element increases, the grain size can be expected to decrease in the  $\alpha$ -aluminium-Phase. With longer reheating time, as a result of maturing processes grain growth can be expected to occur. Apart from that, a significant interaction between titanium and strontium can be identified, although the effect of strontium alone is only minimal and can be identified as being statistically insignificant. The grain refining effect of titanium is evidently weakened by the addition of strontium.

To indicate the affectability of the grain size, in the following detailed evaluations the titanium and strontium content as well as the reheating time were considered in particular (Fig. 4.3). By the addition of 0.4 % titanium (in the form of AlTi5B1) the grain size can be decreased from ~85 to 65  $\mu\text{m}$ . As the reheating time is

extended grain growth can be expected to occur, however this is inhibited by the addition of titanium. This effect of the grain refiner is also dependent on the strontium content. A systematic positive effect of the manganese and lead addition can not be ruled out. The change in the grain size as a result of grain refining treatment, as well as the effect of the duration of the reheating time with simultaneous modification using strontium, is illustrated in Figure 4.3a.

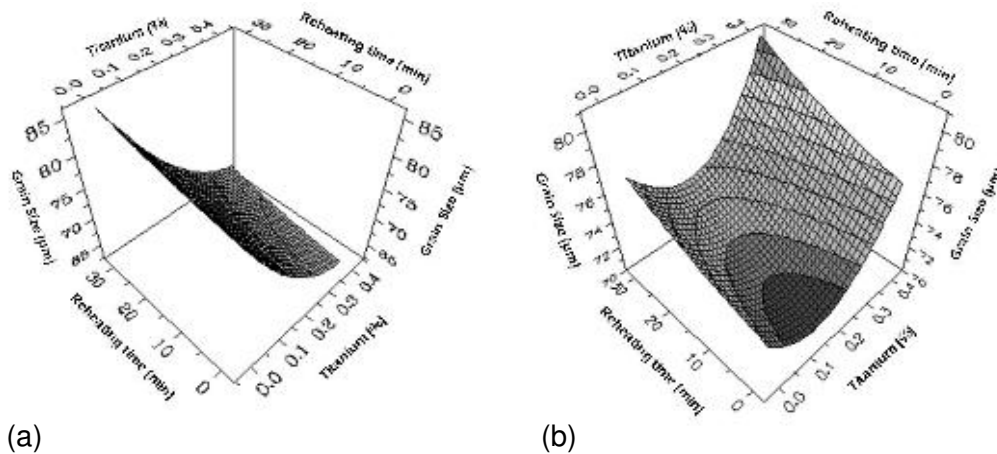


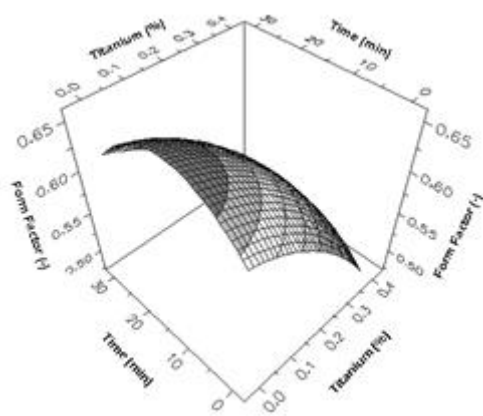
Figure 4.3: Grain size =  $f$  (titanium content, reheating time)

(a) without Sr and (b) with Sr, (b) Modification on the eutectic grain structure depending on the content of Sr (ppm) and Ti.

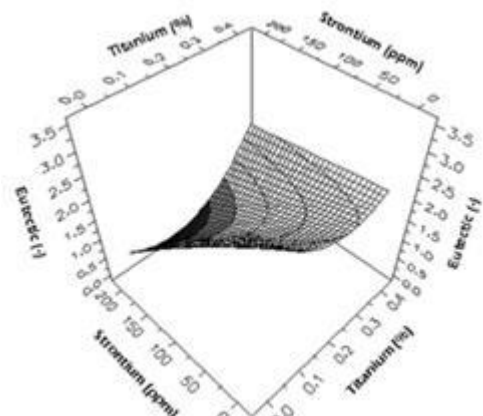
#### 4.2.3 Influence on the Form Factor of the Primary Phase

A further criterion for evaluation in the assessment of thixoforming materials is the form factor. The rounder the grain or the greater the form factor is, the more pronounced the thixotropic material characteristic in a forming operation will become. The duration of reheating is recognised as an essential parameter affecting the form factor. The effect of alloying elements on the forming is however largely unexplained. For the material A356 (EN AC-AISi7Mg0.3), the main parameter affecting the form factor of the primary phase ( $\alpha$ -aluminium) surprisingly appears to be the addition of strontium, which appears to have an even greater effect in comparison with the reheating time. The other elements, on the other hand, cannot be identified as significant parameters. The dependence of the form factor on the titanium added and on the reheating time with manganese added and also modification using strontium is shown in Figure 4.4.





(a)



(b)

Figure 4.4: Dependence of form factor on reheating time and titanium content (0.3 % Mn, 200 ppm Sr, 0 ppm Na, 0 % Pb)

With increasing titanium content the form factor is clearly impaired, i.e. the titanium added during solidification evidently promotes dendritic growth. At the same time the form factor passes through its maximum with extended reheating, lasting between 10 and 20 minutes. After that uneven grain growth occurs, during which smaller  $\alpha$ -aluminium dendrites agglomerate to larger grains, so that the form factor "apparently" becomes worse. Under favourable conditions ( $t = 15 - 20$  min.,  $Ti = 0$  %,  $Pb = 0$  %,  $Na = 0$  %,  $Sr = 200$  ppm) a form factor of  $\sim 0.7$  can be achieved. This also approximately corresponds to the form factor achieved when reheating conventional raw material, for instance when using the MHD process. The result appears to be plausible because during reheating the states of dendrite formation, grain growth due to Oswald ripening and strengthened formation of the networking structure as a result of grain contact and coalescence can be differentiated [15].

The optimum grain structure adaptation is achieved when the dendrites can be transferred into individual globulites. The prospects for success of this treatment are essentially defined by the basis grain structure and the chemical composition [14]. By adding 0.3 mass-% Mn and modification using 200 ppm of strontium, the form factor after 30 min reheating can be favourably affected, because formation of the dendrites into a globulitic form during the same period leads to a better form factor than without manganese and strontium added (Figure 4.5).

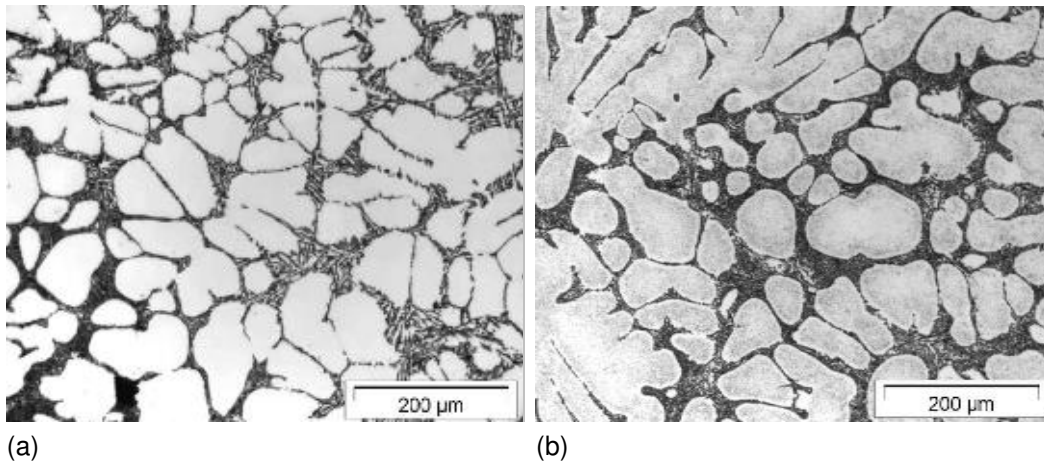


Figure 4.5: Micro structure of A356

(a) without Sr- and Mn-refining ( $f = 0.45$ ), (b) with Sr- and Mn-refining ( $f = 0.55$ )

#### 4.2.4 Modification of the Eutectic Structure

The involvement of the eutectic structure in evaluation of a material's suitability for thixoforming is breaking a new development step. Modification treatment and division of the modification into different classes is on the other hand standard practice for processing of conventional aluminium castings. A grain structure having a very fine, uniformly distributed eutectic represents Class 1. On the other hand coarse, needle-shaped, unevenly distributed silicon precipitations represent Class 3. Silicon precipitations in the intermediate group represent Class 2. Successful modification (Class 1) enhances internal feeding, minimises the porosity as well as the tendency to heat cracking of a material, positively affects the flow and form-filling characteristics and improves the mechanical properties of the component.

The formation of the eutectic grain structure in testing of thixo-alloys can be expected to be primarily affected by strontium. On the other hand, titanium and manganese have very little effect. Due to resulting interactions, alloying elements such as titanium also have a significant worsening effect on the refinement and uniformity of the eutectic if strontium is also present. If strontium is added, titanium should be limited to between 0.15 - 0.25 mass-% (Figure 4.4b). If 0.3 mass-% of manganese is added the negative effect of titanium on modification of the eutectic can be reduced to some extent.

#### **4.2.5 Influencing the Semi Solid Temperature Interval**

Determination of the freezing range for alloys is carried out by means of Differential Thermo-Analysis (DTA). Both the grain refinement and modification should have a favourable effect on the semi solid temperature interval. The liquidus temperature becomes higher with increasing titanium content. In addition, it could be demonstrated that the silicon and magnesium contents, and also the lead content in particular, should also be taken into consideration because the liquidus temperature reacts significantly to the alloying content.

The grain refinement element is primarily suitable in favourably affecting the freezing range overall. All other alloying elements are of little significance in comparison. Lead has a generally negative effect on the freezing range so this element should be avoided. The study confirmed the suitability of the thermo-analysis principle for assessment and control of the melt range. The hoped-for evaluation of the modifying treatment as well as grain refinement by means of thermo-analysis was however not achieved due to the interfering influence of the other alloying components (primarily Mg and Si). The grain-refined raw material differs in comparison to commercial raw materials in respect of its smaller grain size as well as a more uniform grain size distribution in the border and middle areas of the cast. At the same time it was noticeable that the grain-refined raw material had a somewhat more dendritic grain structure composition than commercial raw material.

#### **4.2.6 Characteristics of the Raw Material**

Because the commercially available MHD grain structures and grain-refined raw material can significantly vary from one another after reheating both materials were treated with the same reheating program. The raw materials were heated to the target temperature (580°C) horizontally in an induction unit. The chemically grain-refined raw material was thereby transformed into a fine globulitic grain structure quite as well as for the conventional MHD material. The average grain diameter and the form factor are comparable (Figure 4.6). During reheating however, it was observed that for the chemically grain-refined material less melt ran out of the billet than with conventional raw material. This presents the option that when using grain-refined raw material the dripping losses that are normally incurred during vertical reheating may be reduced.

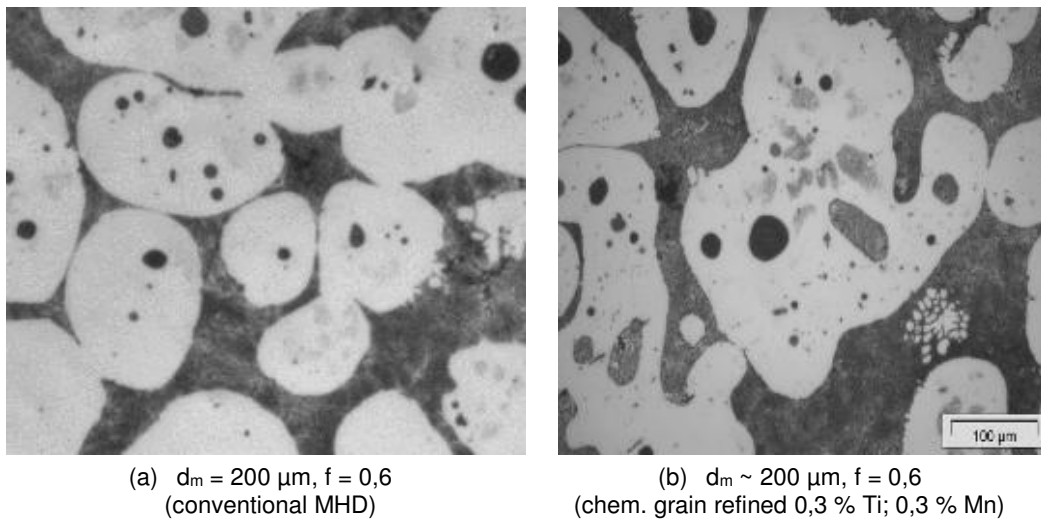


Figure 4.6: Grain structure of the billet centre, A356 after reheating

The reheated raw material is processed in a die-casting forming operation at the foundry institute of RWTH Aachen into principle component (Figure 4.7). A step form is used with which the form filling of a component with decreasing wall thickness can be examined. In contrast to commercial raw material, using chemically grain-refined raw material, with the same form filling rate ( $v_{\text{Piston}} = 0.05 \text{ m/s}$ ) even the overflow of the casting chamber could be filled. This implies that an improved form filling capacity can be achieved.

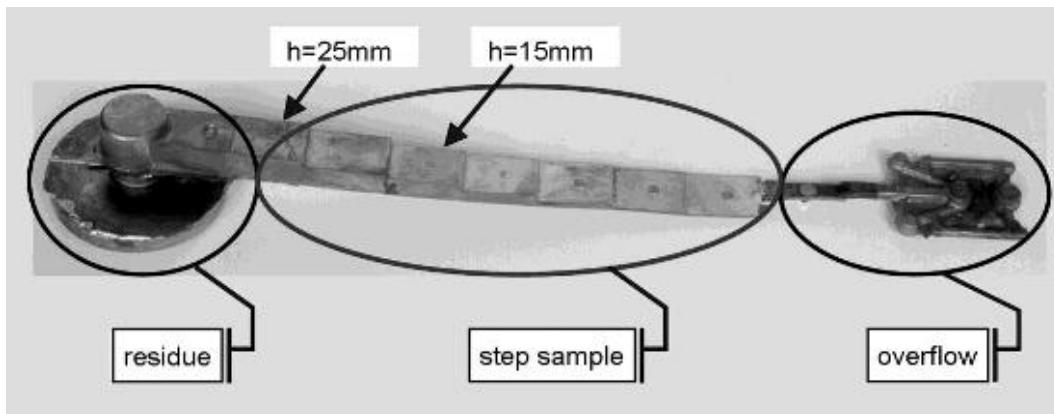


Figure 4.7: Principle step-part made from thixo-adapted A356 (after chemical grain refinement)

Samples were taken from the component out of the steps of 15 and 25 mm height and then metallographic tests were performed (Figure 4.8).

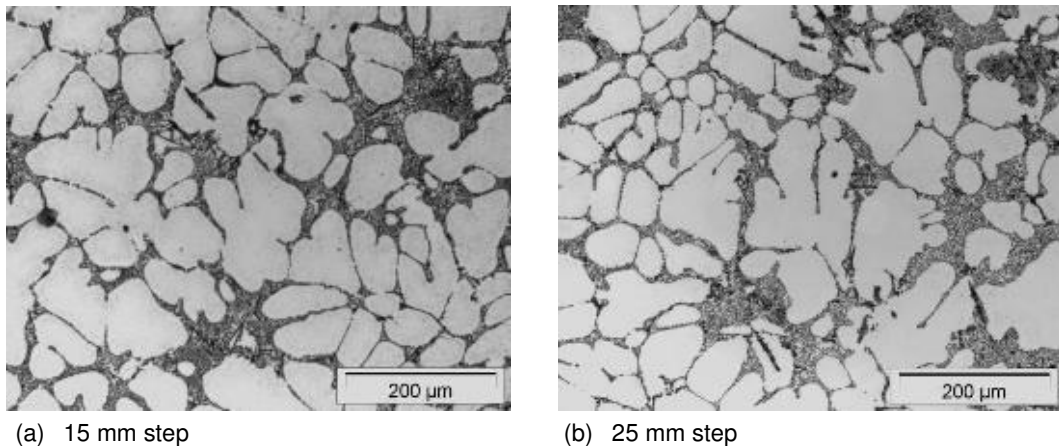


Figure 4.8: Grain structure of thixo-cast step-samples

For both of the raw materials there was no significant variation in grain structure determined in dependence of the step height. The chemically grain-refined material had a somewhat finer grain structure in comparison to the commercial raw material. The advantages that were already apparent in respect of the aluminium phase and eutectic after reheating of the different raw materials were also retained after forming. Examination of the chemical homogeneity over the length of the component indicated that for both raw materials no significant mix separation had occurred.

### 4.3 Fundamentals of Aluminium-Lithium Alloys

#### 4.3.1 State of the Art

Aluminium-lithium alloys have been in use since 1950. In particular wrought alloys such as AA8090 and AA2091 are used in the form of continuous-pressed profiles or rolled sheets in aerospace constructions. Also forged components such as Al-Li brake callipers are used in motor racing [16]. Their low density, high specific solidity and high module of elasticity make these materials highly suitable for a multitude of high-load applications. Because of the high raw material cost of lithium and high expenditure for processing however, they are not very widely used to date. The value of 5 €kg<sup>-1</sup> of tolerable extra costs in transportation systems for reduction in weight per kilogram indicates that their introduction in automotive mass production would only occur if significant cost reductions were feasible.

However, aluminium-lithium alloys are subject to low toughness values, stress-cracking corrosion and heavy anisotropy of mechanical properties [18, 19].

Aluminium-lithium alloys can be produced by melt-technologies and powder-based metallurgical methods. The latter require more complex operating lines (cost issue) but permits a higher lithium content to be applied. However powder-based metallurgy can be subject to high contamination of the powder during the jet-spraying process (e. g. oxide forming - unfavourable for ductility) as well as the high reactivity of the lithium itself. Melt-based metallurgical production is more common but the achievable lithium content is limited to ~10 %. During continuous casting of Al-Li semi-finished products, an aluminium melt (99.5 %) with the slightest Li content will become scratched far more quickly than for a Li-free melt. Li contents of >5 ppm can already give rise to problems during casting, when jet-spray/float systems are used. According to [20], between lithium in the aluminium melt and silicon in refractory material (wall components, jets), a  $\text{LiAlSi}_3\text{O}_8$ -phase should form, which is deposited on the walls of the jet along with the above mentioned oxides formed in the melt ( $\text{LiAlO}_2$  and  $\text{Al}_2\text{O}_3$ ) and this can lead to the casting jets blocking up. In [21] studies were conducted into development of suitable aluminium-lithium alloys for fine casting processes. The casting tests using conventional Al-Li forging alloys identified deficiencies in the casting properties. Furthermore the tendency to thermal cracking remained - and that should be eliminated by means of suitable grain refinement. A cost-effective casting technique may in the future be possible by adaptation of the low-pressure or reverse-pressure die casting process using inert gas.

The main motivation is to evaluate the potential for processing of Al-Li-X alloys in the partially liquid state, because the special processing conditions involved can be expected to produce a significant improvement in the material's properties and at the same time greater scope of formability. The main challenges in the production and processing of aluminium-lithium alloys include

- Hot-tearing susceptibility during the casting process.
- Because of its high reactivity, lithium oxidises very rapidly and needs to be handled very carefully.
- High gravitational separation during casting.
- High rate of waste/high proportion of turnings.
- Corrosion susceptibility (particularly stress-cracking corrosion).
- Recycling issues.

The acceptance of Al-Li alloys is currently limited, which is especially due to doubts in respect of fracture toughness and the fact that the costs are always three times higher than for existing high-strength alloys, probably due to the special requirements during melting and casting.

The alloy systems studied are derived on the one hand from the precipitation-hardened system Al-Li-Cu and on the other from the mixed-crystal strengthened system Al-Li-Mg. As a comparison the commercial alloys AA8090 (Al-Li-Cu-Mg), AA2090 (Al-Li-Cu) and AA1420 (Al-Li-Mg) were included in the study. In solid aluminium at 610°C lithium has a maximum solubility of ~4% (16 at-%). Due to the low density of this element ( $0.54 \text{ g} \cdot \text{cm}^{-3}$ ) every 1 % addition of lithium gives rise to a 3 % reduction in density. Amongst the soluble elements lithium is also noteworthy in that it causes the modulus of elasticity of aluminium to increase markedly (6 % increase for every 1 % added). By formation of the regulated meta-stable  $\delta'$  ( $\text{Al}_3\text{Li}$ ) phase, binary and more complex alloys containing lithium can be hardened, which is coherent with the Al-matrix and has a particularly low mismatch with the Al-matrix. Because of these properties, alloys containing lithium are under development as a new generation of low-density, high-rigidity materials for application in airframes, whereby improvements of up to 25 % in the specific rigidity are possible, thus offering the opportunity for the production of a large range of higher performance aluminium alloys by conventional melt-based metallurgical means. In the aluminium industry, these may also contribute to their resistance to the growing trend toward the application of non-metallic composite materials as structural materials in the aerospace industry [22].

Hardened binary Al-Li alloys primarily suffer from low elasticity and toughness under massive stress peaks that can occur, because coherent  $\delta'$  precipitations are sheared by moving displacements. This can give rise to fractures along the grain boundaries. Correspondingly, this work has focussed very heavily on the study of elements forming suitable precipitations or dispersoids allowing the displacements to be dispersed more homogenously. The alloy systems developed to date are compared in Table 4.2.

Table 4.2: Selection of Al-Li alloys developed to date for the aerospace industry

alloy	Li	Cu	Mg	Zr	others
A2020	1.3	4.5	-	-	0.5 Mn; 0.25 Cd
A2090	1.9 - 2.6	2.4 - 3.0	< 0.25	0.08 - 0.15	-
A2091	1.7 - 2.3	1.8 - 2.5	1.1 - 1.9	0.04 - 0.16	-
A8090	2.2 - 2.7	1.0 - 1.6	0.6 - 1.3	0.04 - 0.16	-
A8190	1.9 - 2.6	1.0 - 1.6	0.9 - 1.6	0.04 - 0.14	-
A8091	2.4 - 2.8	1.6 - 2.2	0.5 - 1.2	0.08 - 0.16	-
A8092	2.1 - 2.7	0.5 - 0.5	0.9 - 1.6	0.08 - 0.15	-
A8192	2.3 - 2.9	0.4 - 0.7	0.9 - 1.4	0.08 - 0.15	-
X2094	1.3	4.5	0.4	0.14	0.4 Ag
1420	2.0	-	5.2	0.11	-

#### 4.3.2 The System Al-Cu-Li

The first commercially applied alloy of this system was A2020. Copper on the one hand reduces the solubility of lithium in its solid state, whereby the precipitation of  $\delta'$  is promoted and on the other hand gives rise to the precipitation of phases, such as the GP zones and  $\theta'$ , as familiar from binary Al-Cu alloys. The alloy A2020 combines high properties of strength at room temperature ( $R_{p0.2}$  of ~520 MPa) with good creep behaviour at temperatures up to 175°C and has a module of elasticity 10 % higher than that of other aluminium alloys. Newer Al-Li-Cu alloys have a lower copper content and higher Li:Cu ratios, of which the best-known example is the alloy A2090. In addition to the  $\delta'$ -phase, this alloy is hardened by means of the hexagonal T1-phase ( $Al_2CuLi$ ). Zircon additives (~0.12 %) are also activated in order to form fine dispersoids of the type  $Al_3Zr$ , which control re-crystallisation and grain size. Another effect of this element is to promote grain formation of the  $\delta'$  precipitations on these dispersoids. Overall zircon increases the properties of strength and toughness [13].



#### 4.3.3 The System Al-Li-Mg

Magnesium reduces the solubility of the lithium, although its effect appears to be strengthening the mix-crystal stability. In alloys containing more than 2 % magnesium and that are heat-treated at relatively high temperatures, a non-coherent, cubic  $\text{Al}_2\text{LiMg}$ -phase is formed. Unfortunately this phase generally does not form at the grain boundaries and has an unfavourable effect on toughness. Therefore, the addition of magnesium does not essentially improve the strength of the binary Al-Li alloys. The alloy 1420 has a relatively low yield limit ( $R_{p0.2} \sim 280$  MPa), however high corrosion resistance [23]. Higher yield limits ( $R_{p0.2}$  of 360 MPa) are achieved in the modified alloy 1421. This alloy contains 0.18% of the expensive element scandium, which forms fine, stable dispersoids of the phase  $\text{Al}_3\text{Sc}$ . This is isomorph with an  $\text{Al}_3\text{Zr}$  structure and it promotes increased strength.

#### 4.3.4 The System Al-Li-Cu-Mg

Examples in this group are A2091, A8090 and A8091. Ageing at temperatures of around 200°C leads to co-precipitation of the semi-coherent phases T1 and S' in addition to the coherent phase  $\delta'$ . The S'-phase ( $\text{Al}_2\text{CuMg}$ ) can not be sheared by displacements and therefore enhances a homogenous dispersal of stresses. Because the nucleus formation of this phase is similarly difficult, Al-Li-Cu-Mg alloys are normally used in T8 state (helicopter support arms made from A8090).

#### 4.3.5 The System Al-Li-Cu-Mg-Ag

The costs of delivering freight into low earth orbit are estimated at  $\sim \text{US\$}8000 \text{ kg}^{-1}$ , so that there is considerable encouragement to reduce the weight of space vehicles by the use of lighter or stronger materials. Therefore, alloys containing lithium come into consideration for welded fuel tanks instead of the conventional aluminium alloys 2219 and 2014. Minimal addition of silver and magnesium significantly improves the properties of strength. For Al-Cu-Li-Mg-Ag alloys with lithium contents of around 1-1.3 % the material's strength results from adding small quantities of Mg and Ag which stimulates nucleus formation for a fine, hardened T1-phase which coexists alongside the S' and  $\theta'$  in a maximally hardened state. Each of these precipitations is created in another Al-matrix plane and is resistant to shearing due to displacements. These observations have lead to the development of an alloy known as Weldalite 049 ( $\text{Al-6.3Cu-1.3Li-0.4Mg-0.4Ag-0.17Zr}$ ). This material can have strength characteristics in excess of an  $R_m$  of 700 MPa in the T6 and T8 state. On the basis of the strength/density ratio

corresponding steel would need strength in excess of 2100 MPa, so Werdalite 049 is the first aluminium alloy produced from conventional casting blocks to be designated as having ultra-high strength. Modifications to this alloy using a low copper content (X2094 and X2095) develop values of  $R_{p0.2}$  of ~600 MPa in the T6 state, which is double that of the conventional aluminium alloy 2219-T6 [22].

The original objective for the development of Al-Li-Cu-(Mg) alloys was as a substitute for the conventional aluminium airframe alloys, with an expected density reduction of about 10% and increase in rigidity of 10-15%. These alloys are classified as high-strength (A2090, A8091), medium-strength (A8090) and damage-tolerant (A2091, A8090) in respect of their mechanical properties. Their densities range from 2.53 to 2.60 g/cm<sup>3</sup> and module of elasticity from 78 to 82 GPa. Nevertheless problems do exist in respect of their low lateral toughness in continuously cast profiles. These problems appear to relate to their microstructure, primarily in the grain boundary areas. Under continual loading of these alloys at increased temperatures (>50°C) the incidence of creep-fracturing can also increase to a relatively high degree [24].

#### **4.3.6 Effects of Alkaline Metal Contaminants**

One known factor that reduces the ductility and fracture toughness of alloys containing lithium is, alongside hydrogen, the presence of alkaline metal contaminants (in particular sodium and potassium) and particularly at the grain boundaries. In conventional aluminium alloys these elements are combined with elements such as silicon in harmless, permanent compounds. However they react readily with lithium. Commercial alloys containing lithium are produced by conventional melting and casting techniques and usually contain 3-10 ppm of alkaline metal contaminants. This level can be reduced to below 1 ppm by means of vacuum melting and refining [25]. It can be demonstrated that this leads to a considerable improvement in fracture toughness at room temperature (Figure 4.9).

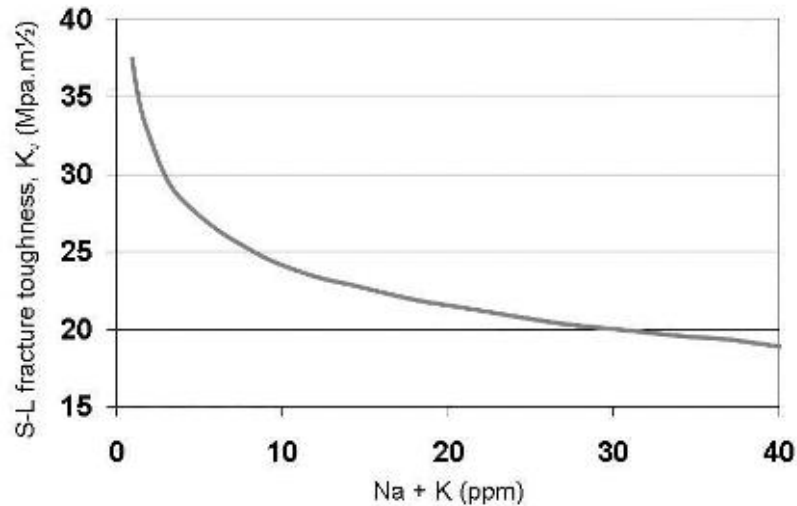


Figure 4.9: Effect of alkaline metal contaminants on the crack toughness on A2090 extruded profiles [26]

#### 4.4 Development of Aluminium-Lithium-Alloys for Semi-Solid Processing

The concept for adaptation/optimisation of familiar Al-Li alloys for processing in a partially liquid state is essentially based on the following points:

- Influencing the micro-grain structure and the texture properties by suitable selection of the composition and the process sequence.
- Optimisation of the degree of recrystallisation and the grain size in relation to the applicable component geometry.
- Adaptation of the casting grain structure by addition of elements such as Ce, Sc, Ti, B and Ag.
- Minimisation of the proportions of balancing phases T2 and  $\delta$ , of Fe and Si phases, of Na and K as well as hydrogen in solution.
- Variations in the main alloying elements (Li, Mg, Cu, Sc, etc.).

The semi-empirical methodology and sub-operations employed are shown in Fig. 4.10. After selecting suitable AL-Li-X basis systems, first an evaluation was made of the important key parameters for processing in a partially liquid state, with the aid of thermochemical calculations. After tuning of the alloys by means of micro-alloying element additives and melt-based metallurgical synthesis of trial alloys as well the characterisation was performed. Finally thixocast and rheocast principle parts and real components were jointly produced and evaluated. Where necessary an adaptation of the selected alloy composition was carried out as well as repeating of the development operation for reproducibility check.

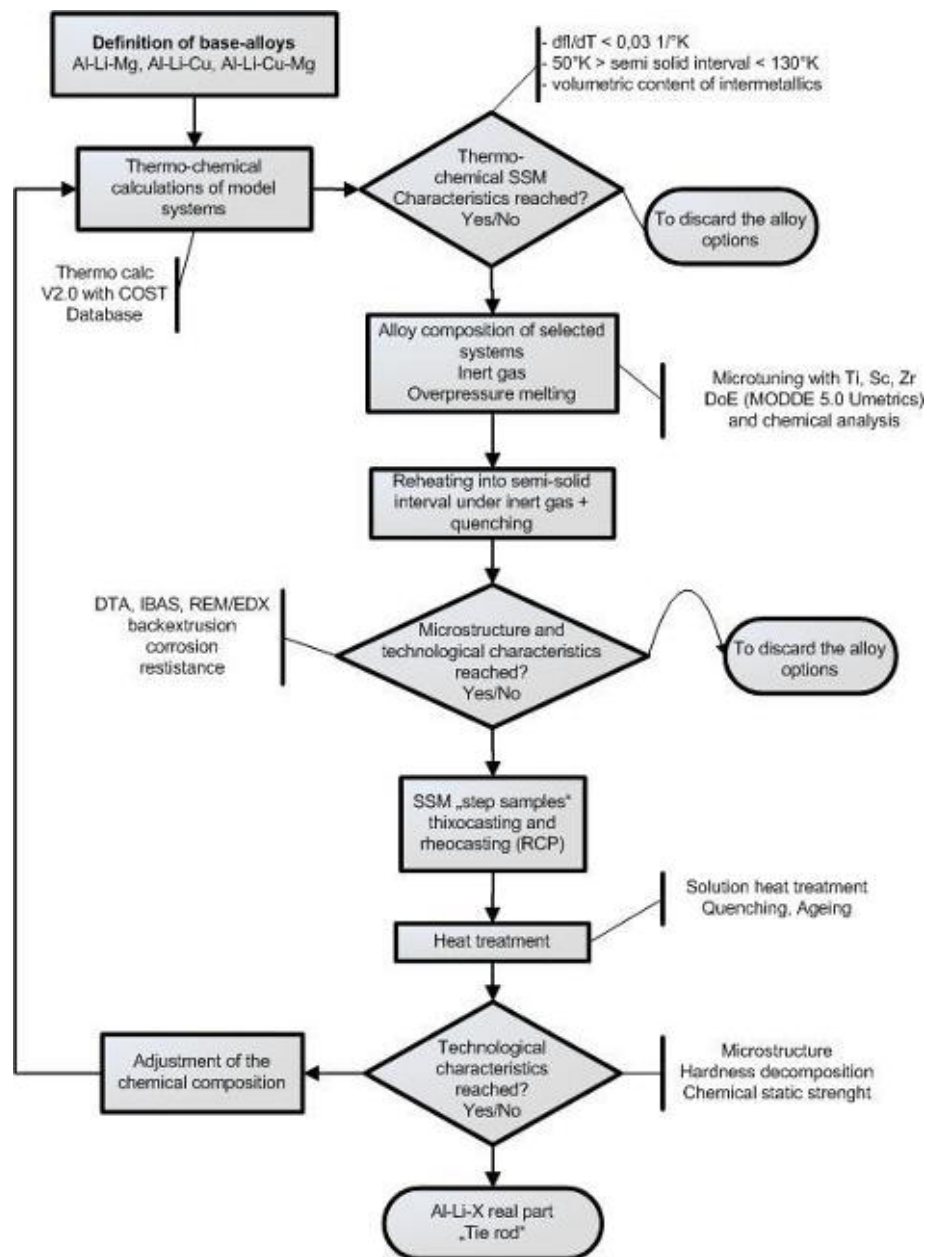


Figure 4.10: Flow diagram of the methodology applied for adaption of Al-Li-X alloys to thixoforming

#### 4.4.1 Thermochemical Modelling

The thermochemical calculations in the selected Al-Li-X system models [27], [28], [29] produced the following results, compared with experimental data [30]:

- In the Al-Li-Cu system the alloys  $\text{AlLi}_4\text{Cu}_4$  (A3) and  $\text{AlLi}_{2.5}\text{Cu}_4$  (A2) display the lowest temperature-sensitivity in the liquid phase portion. Both are below the critical value of  $df_l/dT < 0.015$  for a liquid phase proportion of 50% and therefore should be suitable for processing in the semi-solid range. The alloys  $\text{AlLi}_{2.5}\text{Cu}_{2.5}$  (A1) and  $\text{AlLi}_4\text{Cu}_{1.5}$  (A4) display a smaller processing window in relation to temperature-sensitivity of the liquid phase portion, however should prove of interest for processing with low liquid phase proportion (<30%) for thixoforging.
- In the Al-Li-Cu system account must be taken of the occurrence of brittle intermetallic phases  $\text{T2-Al}_5\text{CuLi}_3$  and  $\text{T1-Al}_6(\text{Cu,Zn})\text{Li}_3$ . This could in some cases lead to worsening of the mechanical properties, in particular elongation.
- In the Al-Li-Mg system the alloys  $\text{AlLi}_4\text{Mg}_8$  (A7) and  $\text{AlLi}_{2.1}\text{Mg}_{5.5}$  (A8) display the lowest temperature-sensitivity in the liquid phase portion. Both are below the critical value of  $df_l/dT < 0.015$  for a liquid phase proportion of 50% and therefore should be suitable for processing in the semi-solid range. Similar to the argument for A1 and A4, the alloy  $\text{AlLi}_{2.5}\text{Mg}_4$  (A6) should be suitable for processing with low liquid phase proportion (<30%) for thixoforging.
- In the Al-Li-Mg system account must be taken of the occurrence of the brittle intermetallic phases  $\sigma\text{-AlLi}$  and  $\text{T-Al}_2\text{LiMg}$ , in particular for the alloy A7.
- The complex alloy in the system Al-Li-Mg-Cu ( $\text{A5-AlLi}_{2.1}\text{Cu}_{1.2}\text{Mg}_{0.7}$ ) is excluded due to a insufficient process window for semi-solid forming.

The important key parameters on the basis of the thermochemical calculations are summarised in Table 4.3.

Table 4.3: Properties of selected Al-Li-X alloys relevant to SSM processing, calculations made by Scheil-Gulliver approximation (alloying content in weight%)

alloy	Cu (w/o)	Li (w/o)	Mg (w/o)	T <sub>50</sub> (°C)	df/dT	T <sub>50</sub> -T <sub>s</sub> (°C)	intermetallic phases
A1 (AA2090)	2.5	2.5	-	637	0.023	105	4.7 % T <sub>2</sub> , 1 % T <sub>1</sub>
A2	4.0	2.5	-	629	0.015	97	4.8 %T <sub>2</sub> , 2.7 %T <sub>1</sub> , 0.3% T <sub>B</sub>
A3	4.0	4.0	-	605	0.008	39	12.5 % T <sub>2</sub> , 0.6 % AlLi
A4	4.0	1.3	-	639	0.024	107	2.5 % T <sub>1</sub> , 2.1 % T <sub>B</sub>
A5 (AA8090)	1.2	2.5	0.7	638	0.026	197	3.3 % T <sub>2</sub> , 0.5 % AlLi, 0.4 % $\tau$
A6	-	2.5	4.0	613	0.012	155	5.2 % $\tau$ , 2.7 % $\gamma$
A7	-	4.0	8.0	542	0.004	84	15.5 % $\tau$ , 5.9 % $\gamma$ , 1.1 % AlLi
A8 (AA1420)	-	2.1	5.5	603	0.010	145	3.4 % $\tau$ , 5.2 % $\gamma$

#### 4.4.2 Choice of a Suitable Basis System

Since for semi-solid workability the formation of a globulitic microstructure is a prerequisite quench tests were carried out from the partially liquid range. The average solid phase particle diameter should be less than 100  $\mu\text{m}$  in this respect. The grain structure formations indicate that the grain-refined alloys A1, A2, A4 and A5 formed the larger globulitic particles with virtually identical solid phase contents. The alloys A3, A6, A7 and A8 on the other hand display the desired grain sizes (<100  $\mu\text{m}$ ). The alloys A3 and A7 from this group were taken as samples for detailed examination, because these displayed the largest semi-solid ranges and a finer globulitic grain structure.

With the AlLi<sub>4</sub>Cu<sub>4</sub>(A3) alloy, in the following quench tests were carried out based on 540°C to 620°C after holding times of 2, 5, 10 and 20 minutes. For each quenched sample, four recorded grain structure images (Figure 4.11) were evaluated. The liquid-phase portion at above 540°C is independent of the holding time in this respect. The liquid phase progressions for a holding time of 2

minutes, determined on the basis of the quench tests, were very closely consistent with the DTA results. The mean grain sizes (600°C) amount to 60 to 80 µm and remain very constant up to a holding time of 20 minutes. The form factor at 600°C, with values of 0.5 to 0.6 is more favourable than at 590°C (0.35 to 0.45), because more solid phase is released and therefore a higher form factor is created. This means there is a process window as indicated in Table 2.3.6. The stated temperatures vary because of the non-homogenous alloy distribution within a billet.

With the AlLi4Mg8-(A7) alloy analogue quench tests were performed based on 460°C to 580°C. As for AlLi4Cu4 (A3) there is no indication of any significant interdependence between the liquid phase portion and the holding time. Again there is a good correlation of the liquid phase contents determined by both DTA and quench tests. The mean grain sizes vary at both temperatures, between 35 and 65 µm, the form factor between 0.37 and 0.48. Because of its grain structure, the examined material is therefore suitable for processing in the semi-solid state. Because of the large fluctuations in relation to the chemical compositions, it is difficult to identify a definite process window for the material on the basis of the DTA and grain structure tests (assumed:  $T_{\text{process}} \sim 540^{\circ}\text{C} \pm 15^{\circ}\text{C}$ ,  $t_{\text{hold}} \sim 2\text{-}5\text{ min}$ ). A higher homogeneity would be necessary for reproducible billet heating.

#### **4.4.3 Fine Tuning of the Grain Refinement for Al-Li-Alloys**

For statistically confirmed determination of the parameters and effect variables during micro-tuning of the Al-Li-X alloys by means of adding Sc and Zr, the model-supported testing plan was carried out using software type MODDE 5.0®. The parameters for Sc and Zr content, as well as the casting temperature, were defined for the system AlLi2.1Mg5.5. The indicator (effect variable) was the desired average grain size in the cast billets, which should be minimised.

As shown in Figure 4.12, the effects of added Sc and Zr on the resulting grain size are significant. The variation of the casting temperature on the other hand has no effect on the grain size. The grain size can be statistically confirmed and reproducibly set at the desired value via the Sc and Zr contents. Figure 4.13 shows in this respect which contents of Sc and Zr have to be added in order to set a defined grain size in the alloy. The mathematical model makes a prognosis of contents of 0.25 % Sc and 0.25 % Zr for a grain size of 30 µm.

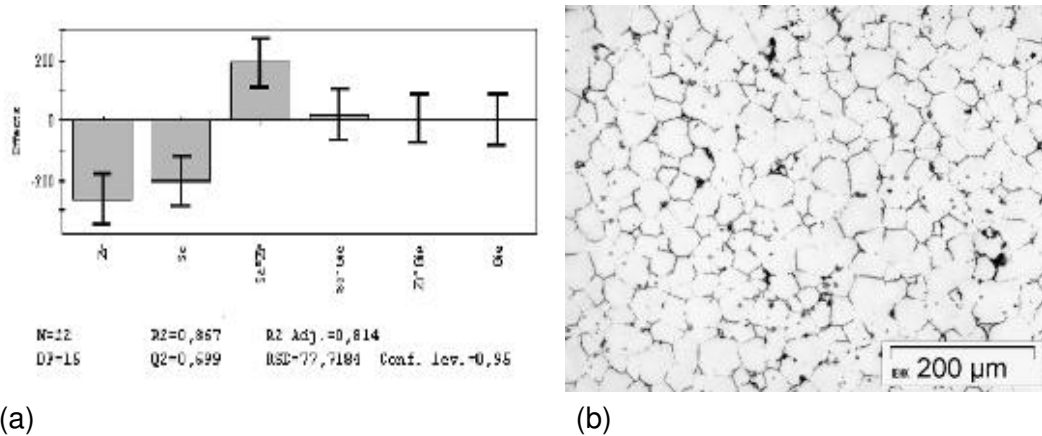


Figure 4.12: Effects of Sc and Zr and casting temperature on the grain size of AlLi<sub>2.1</sub>Mg<sub>5.5</sub>ScZr (a) and micro structure of a billet (b)

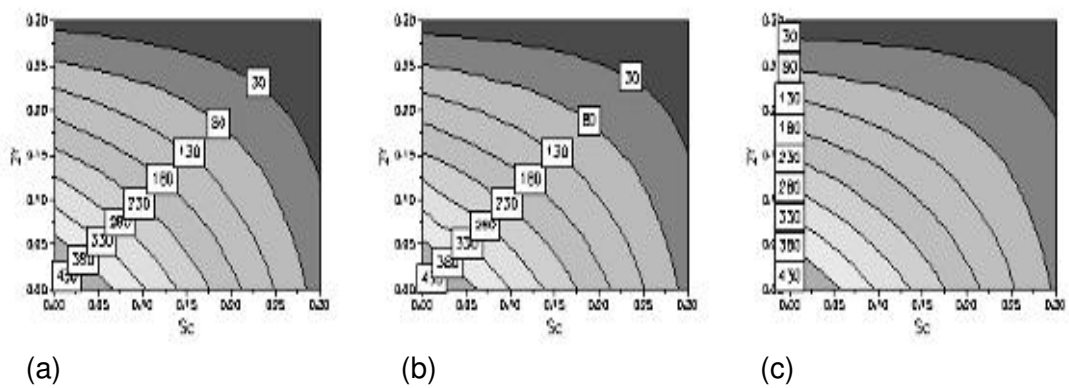


Figure 4.13: Dependence of the average grain size in μm (white boxes) on the Sc and Zr contents of AlLi<sub>2.1</sub>Mg<sub>5.5</sub>ZrSc at three casting temperatures (a) 750°C, (b) 800°C, (c) 850°C

#### 4.4.4 Assessment of the Raw Material Development Programme

The results of the optimization programme can be summarized as follows:

- With the aid of the overpressure melt process Al-Li-X alloys with Li contents of 1.5 - 4 weight% can be reproducibly produced. In order to prevent contamination by Na and K, it is necessary to employ master alloys and high grade metals.
- In spite of the complex permanent mould system, chemical non-homogeneity of the raw material billet can not be entirely eliminated. In



particular the elements Cu and Mg are concentrated at the edge of the billet and are below the specified desired values in the centre of the billet.

- DTA testing confirmed the results of the thermochemical calculations, whilst for the  $\text{AlLi}_4\text{Cu}_4$ ,  $\text{AlLi}_4\text{Mg}_8$  and  $\text{Al-Li}_{2.1}\text{Mg}_{5.5}$  alloy systems the largest process window for processing in the semi-solid range can be expected.
- The evaluations for the micro structure in the semi-solid range indicate that in particular the Ti and Zr grain-refined alloys  $\text{AlLi}_4\text{Cu}_4$  and  $\text{AlLi}_4\text{Mg}_8$  as well as the Sc and Zr micro-alloyed alloys  $\text{AlLi}_{2.1}\text{Mg}_{5.5}$  achieve very good results with globular and fine-grained structures of  $\sim 60\text{ }\mu\text{m}$ . Apart from that, these alloys have a high proportion of pre-melting eutectic phase, which should support thixotropic flow during forming.

#### **4.5 Consideration of the Forming Pressure on Thixoalloy Development**

For full consideration of the process window during forming in the partially liquid state, solidification under pressure has to be taken into consideration, because at the end of the forming process pressures of up to 1000 bar can be reached. This effect calls for changes in the phase transformation temperatures and considerable shifting of phase state ranges, even the occurrence of new phases and modified solubilities for the alloying elements. Preliminary metallurgical studies regarding the effect of the pressure on the properties of metals and alloys solidified under pressure indicate that alloys solidified under these conditions possess greatly enhanced mechanical properties. This effect must be taken into account for the solidification of alloys in the partially liquid state, in particular for aluminium alloys because the elevated pressure has a great influence on the solidification temperature of the residual melt and so, due to the sudden solidification (pressure-induced under-cooling), non-homogeneity of the component can be the result. The pressures building up in the partially liquid state during the forming process can however have a positive effect, e.g. considerable improvement of mechanical properties. Therefore pressure, forming rate and temperature control must be adapted to each other in order to produce homogenous components with enhanced mechanical properties.

When continuously casting Al-Si raw material for thixoforming by means of electro-magnetic agitation (MHD), in near-surface regions of the rod an increase in the silicon content occurs in comparison with the core area [36]. For the most widely used thixo-alloy  $\text{AlSi}_7\text{Mg}$  the silicon content close to surface can even increase to an over-eutectic level if the agitating effect is very strong. The cause may for instance be a shifting of the eutectic point due to the overpressure [37].

This leads to non-homogeneity in subsequently produced thixocast components. It is recognised from literature as well as from own experience that in the case of re-melting of the surface regions, when a shrinkage gap is created a transfer of eutectic residual melt in the edge area is possible through the framework of the primary crystal structure, if an overpressure is acting internally ([38] and [39]). However these studies only give information about the effect of pressures of up to ~10 bar. For a comprehensive understanding of the effects of pressure, in particular for thixoforming, it is not sufficient to limit oneself to such a low level of pressure.

During component production by thixoforming as a rule final pressures of about 1000 bar are created, which influences the still liquid phase portion of the suspension. As mentioned above, this effect calls for changing of the phase transformation temperatures as well as considerable shifting of phase state ranges, even the occurrence of new phases and modified solubilities of the alloying elements. Cernov and Schinyaev [40] have already published a pressure dependency of this nature, although this was purely theoretical and derived from the Clausius-Clapeyron equation under the assumption that the heat of the melt and the volume change during melting are constant, i.e. independent of pressure and temperature. Experimental validation of this is insufficiently covered. In [37] it is postulated that for a shift of the eutectic composition, of for instance the Al-Si eutectic, from 12.6 % to 13.6 %, an absolute pressure of well over 1000 bar would be necessary. However, even at low pressures an extension of the melt range occurs as well, similarly of the solubility range of the aluminium solid solution. Therefore, particularly during forming under pressure in the partially liquid state, large effects can be expected on the grain structure composition.

For some Al alloy systems the effects of solidification under pressure on mechanical properties were studied [41]. For the system Al-Mg<sub>10</sub>, for example, considerable increase in the yield limit, tensile strength and elongation was indicated with increasing solidification pressure at pressures up to 1000 bar. For the conventional casting alloys A356-AlSi7Mg on the other hand the solidification pressure had little effect on mechanical properties. The works to date studying the influence of pressure on the properties of metals are related to solidification from the fully liquid state. No studies are known that have dealt with the solidification of partially liquid suspensions under pressure. This question is, however, of particular importance for this task, being one of the possible causes of chemical non-homogeneity in thixo-components, and this underlines the need for this research.

#### **4.5.1 Experimental**

The alloys being studied for pressure-dependency were selected from the binary Al-Mg-system (samples 1-4), from the binary Al-Li system (samples 5-8) and from the ternary Al-Li-Mg system (samples 9-17), this allowed for a good of the relevant Al domain (Figure 4.14).

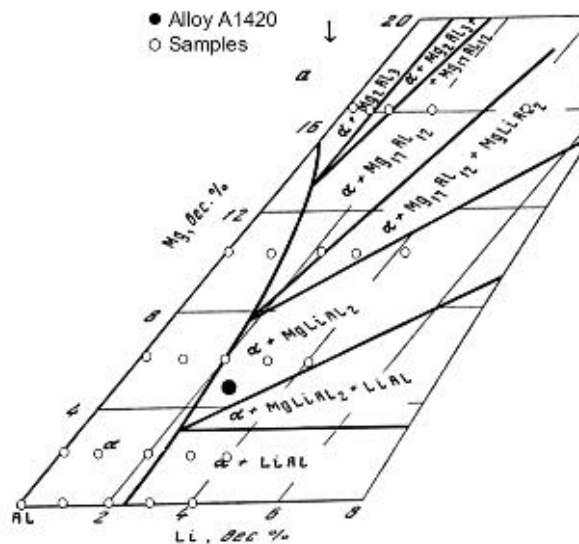


Figure 4.14: Alloy compositions in the Al-Li-Mg system selected for determination of pressure-dependence

For the production of the selected alloys the proven inert gas overpressure method was used. Synthesis of the various Al-Li alloys was carried out by the melt-based metallurgical process directly, from highest purity metals (Al 99.999 %, Li 99.8 % and Mg 99.8 %). The castings were produced with an overpressure in the furnace in a circular steel permanent mould (D = 80 mm/H = 220 mm). The weight of the Al-Li-X trial billet produced was ~2.8 - 3 kg. In order to check the homogeneity of the billets produced, selected billets were sampled at four different levels (in total 12 samples per billet). The deviations in the central regions of the billets were minimal compositions in the edge areas amounted to 5 – 9 % for Mg content and 15 – 25 % for Li content in relation to the desired value. The deviations in the central regions of the billets were minimal. For this reason the samples for the DTA testing (six samples: Ø = 10 mm, L = 60 mm per billet) were taken from the central regions, from the two billets containing 1 % Li as well as containing 2 % Mg/1 % Li. Also it was not possible to take the samples 10 % Mg/4 % Li, 16 % Mg/0.5 % Li, 16 % Mg/0.7 % Li, 16 % Mg/2 % Li, 16 % Mg/4 % Li as they were so brittle that they broke during handling of the samples.

The samples were investigated in a specialized DTA system at pressures from 1 to 2000 bar. The samples contained an ~1.2 mm hole for a thermo-couple. Three other thermo-couples assured the homogeneity of the temperature within the furnace surrounding the sample. The chamber was evacuated and an argon pressure of 15 - 20 bar was applied in order to improve heat transfer. The samples were heated to ~780°C and for measurements under "normal conditions" they were cooled down (at 3 – 5°C/min) for solidification.

For recording of the DTA curves under high pressure a pressure of 2000 bar was applied on the hot sample solidified again at the same rate of cooling. Two tests were run for each billet. After DTA analysis the samples and two untreated samples per billet were used for tensile strength testing.

#### **4.5.2 Results of High Pressure DTA**

The results generally indicate that for almost all samples solidified under a pressure of 2000 bar (exception sample 6), a substantial increase in the liquidus temperature was identified (Table 4.5). Figure 4.15 shows examples of DTA recordings for the Al<sub>3</sub>-Li sample under normal pressure and under 2000 bar, all results are summarized in Table 4.5.

The effect of the pressure on the increase of the liquidus temperature is most significant in the binary systems Al-Li ( $\Delta T = 16.2$  to  $47.4^\circ\text{C}$ ). In the binary systems Al-Mg the pressure effect is somewhat less ( $\Delta T = 16.2$  to  $24.2^\circ\text{C}$ ), similarly for the ternary system Al-Li-Mg ( $\Delta T = 7.2$  to  $23.2^\circ\text{C}$ ). A systematic correlation between the pressure effect on the increase of the liquidus temperature and the structure of the corresponding binary and ternary systems could not so far be identified.

Table 4.5: Liquidus temperatures of alloys solidified under normal pressure and under 2000 bar, determined by means of DTA

sample No.	composition weight-% / atom.-%			T <sub>Liquid</sub> normal pressure (°C)	T <sub>liquid</sub> 2000 bar (°C)	$\Delta T$ (T <sub>Liquid, 2000 bar</sub> – T <sub>Liquid, 1 bar</sub> ) (°C)
	Al	Mg	Li			
1	98 / 97.8	2 / 2.2	0	625.4	649.6	24.2
2	92 / 93.23	6 / 6.75	0	615.2	626.9	11.7
3	90 / 89	10 / 11	0	588.1	600.9	12.8
4	84 / 82.5	16 / 17.5	0	541.1	562.7	21.6
5	99 / 96.2	0	1 / 3.8	635.7	651.9	16.2
6	98 / 92.6	0	2 / 7.4	627.3	620.8	-6.5
7	97 / 89.3	0	3 / 10.7	596.9	644.3	47.4
8	96 / 86.1	0	4 / 13.9	590.6	628.3	37.7
9	97 / 94.1	2 / 2.2	1 / 3.8	631.3	646.1	14.8
10	96 / 90	2 / 2.0	2 / 7.3	623.5	632.5	9.0
11	95 / 87.3	2 / 2	3 / 10.7	612.4	626.5	14.1
12	94 / 84.1	2 / 2	4 / 13.9	600	623.2	23.2
13	93 / 89.8	6 / 6.4	1 / 3.8	568.7	587.2	18.5
14	92 / 86.4	6 / 6.3	2 / 7.3	601.3	611.0	9.7
15	91 / 83.2	6 / 6.1	3 / 10.7	585.6	613.5	27.9
16	90 / 80.2	6 / 5.9	4 / 13.9	573.1	598.5	25.4
17	89 / 85.6	10 / 10.7	1 / 3.7	584.9	592.1	7.2
27	96.4 / 92.3	2.1 / 2.2	1.46 / 5.4	610.4	635.7	25.3

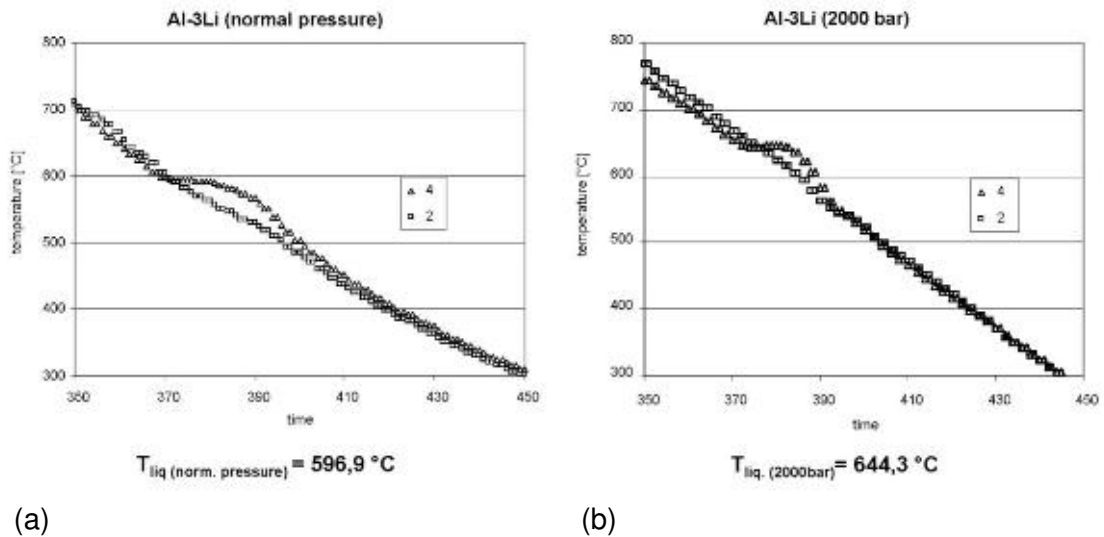


Figure 4.15: Examples of DTA records under normal and under high pressure showing differences in the thermal effect (liquidus temperature at 597°C/644°C)

#### 4.5.3 Effect of the Solidification Pressure on the Microstructure

All samples that were solidified under a pressure of 2000 bar were very brittle, which is due to a phase modification and/or dissolution of a brittle phase on the phase boundaries. An analysis of the micro structure indicates that the morphology of the phase changes and that non-metallic contamination has accumulated at the phase boundaries of the sample that was solidified at 5-8 K/s under pressure (Figures 4.16 and 4.17).

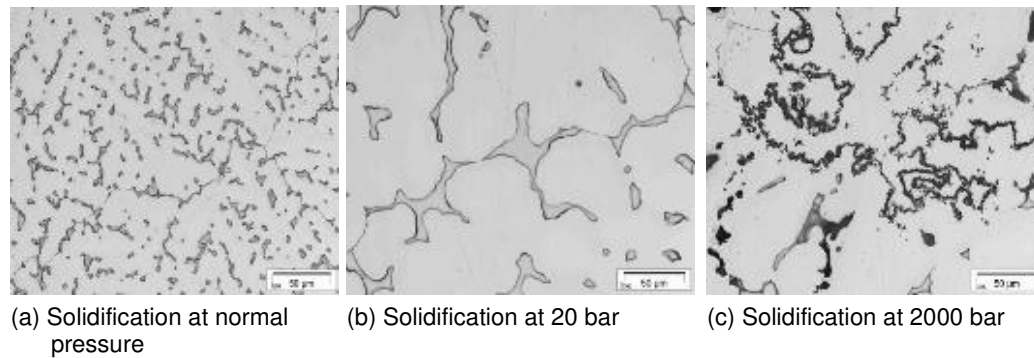


Figure 4.16: Microstructures of Al-10Mg-1Li solidified under different pressures

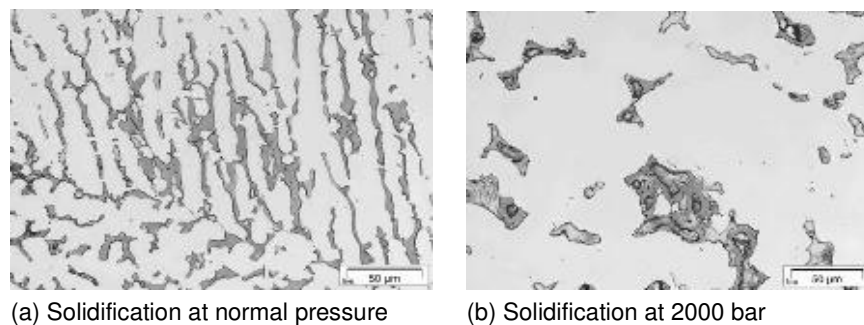


Figure 4.17: Microstructures of Al-6Mg-4Li solidified under different pressures

In the samples solidified under normal conditions, the intermetallic inclusions are uniformly finely distributed within the alloy matrix, whilst in the samples solidified under a pressure of 20 bar, these intermetallics are separated irregularly in a coarser form (Figure 4.16). In the samples solidified under a pressure of 2000 bar, the separation of the intermetallic is somewhat less again and at the phase boundaries as well as between the mix crystals the non-metallic contamination is eliminated (Figures 4.16 and 4.17, both on the right). As the used high-purity argon (6.0) 0.2 vol.-ppm still contains oxygen and the fact that during compression to 2000 bar this content increases to 400 vol.-ppm, the oxide phase formation in the highly reactive Al-Li-Mg alloys is understandable. The solubilities of Li and Mg in the aluminium-mix crystal that were increased under pressure and the formation of non-metallic contamination are responsible for the reduced

mechanical properties of the samples solidified under pressure. By using oxygen-free argon and applying heat treatment this negative effect could possibly be reduced.

#### 4.5.4 Possible Impacts of High Pressure for the Thixoforming Process

The cooling curves for Al-Mg-Li alloys under 2000 bar indicate that the pressure has a very great influence on the melting temperature of these alloys. Increases in the liquidus temperature of up to 47°C were identified. This has a direct effect on the distribution of the alloying elements and on the liquid/solid phase proportion. This effect is shown exemplarily of an Al-4 % Mg-2.1 % Li-0.8 % sample/alloy (Figure 4.18).

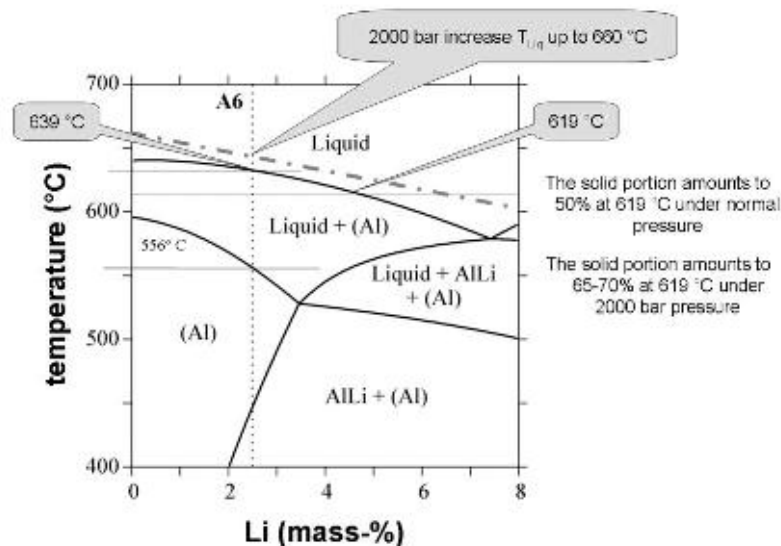


Figure 4.18: Al-Li-Phase diagram showing the change of the fluid/solid phase distribution

Under normal pressure, this alloy has a freezing range of 83°C ( $T_{\text{Liquidus}}$  639°C,  $T_{\text{Solidus}}$  556°C). A 50% liquid phase fraction is achieved at 619°C, corresponding to an under-cooling of the melt by 20°C. During forming of the suspension the pressure raise suddenly and a pressure of, for instance, 2000 bar increases the liquidus temperature by 25.3°C. Merely due to the rise in pressure the under-cooling changes from 20°C to 45.3°C. This high value of under-cooling leads to the formation of an additional solid phase portion. Such the process requires a considerable displacement in the process window. This phenomenon, which also takes place to a slight degree at low pressures [37], can cause increases in alloying elements in the component as well changes in viscosity.

## 4.6 Preparation of Principle Components from Al-Li Thixoalloys

### 4.6.1 Thixocasting

On the basis of the thermochemical calculations, DTA analyses and grain structure characterisation in the partially liquid state, two compositions of the Al-Li system were defined as having the greatest potential for thixocasting. Both have a lithium content of ~4.0 weight%. One alloy contains ~4.0 weight% of magnesium and the other ~4.0 weight% of copper, each with low amounts of added titanium and zircon. The objective of this part of the study was also to prepare a suitable heating strategy for inductive heating of the reactive aluminium-lithium alloys. Pyrometallurgically produced Al-Li billets (diameter 80 mm, length 200 mm) were mechanically cleansed of external oxide layers and macro-cavities. With reference to the thermochemical calculations and the DTA testing completed with the heating experiments a suitable process temperature could be specified for both alloys (Table 4.6)

Table 4.6: Process window for the alloy A3 and A7

<b>A3</b>	$T_s$	$\approx 550 - 560^\circ\text{C}$	$T_L$	$\approx 660 - 679^\circ\text{C}$
	$T^{40-60}$	$\approx 590 - 610^\circ\text{C}$	$\Delta T^{40-60}$	$= 20\text{K}$
	$T_{\text{process}}$	$\sim 590 - 600^\circ\text{C}$	$t_{\text{hold}}$	$= 2 - 5 \text{ min}$
<b>A7</b>	$T_s$	$\approx 460 - 470^\circ\text{C}$	$T_L$	$\approx 650 - 660^\circ\text{C}$
	$T^{40-60}$	$\approx 530 - 560^\circ\text{C}$	$\Delta T^{40-60}$	$= 30\text{K}$
	$T_{\text{process}}$	$\sim 530 - 550^\circ\text{C}$	$t_{\text{hold}}$	$= 2 - 5 \text{ min}$

In respect of the high reactivity of the alloys the raw material billets were packed in a foil of high-purity aluminium for inductive heating; this in order to reduce any contact with the atmosphere as far as possible. When using the protective aluminium foil there is no need for additional purging of the basin with inert gas during heating. The 3" billets were heated to the partially liquid state within a period of 420 seconds, with a solid phase proportion of 50 %. A billet format (diameter 76 mm, length 160 mm) suitable for the horizontal heating system was used. The state of the partially liquid billets was first subjectively estimated by manual cutting. For the alloy AlLi4Mg8Ti a very good processing state was achieved at  $562^\circ\text{C}$ , whilst the alloy AlLi4Cu4Ti first displayed a suitable cutting characteristic at  $\sim 601^\circ\text{C}$ . At the end of the homogenizing phase both materials had a temperature difference between the edge and the centre of  $\sim 1.5^\circ\text{C}$ .



During the practical examinations it could be demonstrated the metal alloyed with magnesium (AlLi4Mg8Ti) can even be safely heated in the partially liquid state without the protective foil. The alloyed magnesium gives rise to an oxidation layer forming on the surface of the billet, thus greatly inhibiting any further ingress of oxygen. After inductive reheating the partially liquid billet was manually transferred in a ceramic carrier basin and placed in the preheated casting chamber (Foundry Institute of RWTH Aachen). The effect of the solidification rate (wall thickness 1 – 25 mm) on the casting grain structure was studied by casting into a step form (Figure 4.19). The form was preheated to a temperature of ~250°C using 3 heater-cooler units. When the component was removed from the too early ignition of the casting residue took place that was still in a partially liquid state. During removal from the form some of the thinner component walls cracked. In general the alloy AlLi4Mg8Ti displayed better flow characteristics and visual surface quality than that of the alloy AlLi4Cu4Ti.

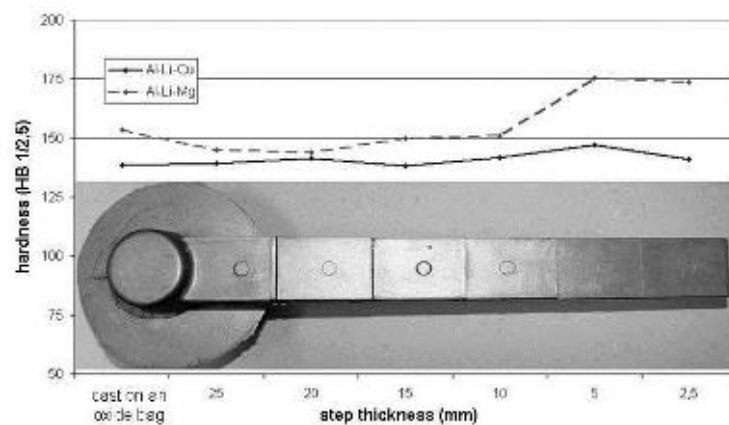


Figure 4.19: Hardness development of step samples derived from an Al-Li-X principle component

Figure 4.20 shows the grain structure of the 25 and 2.5 mm steps for both materials. Both materials display a virtually perfect thixo-grain structure with a pronounced globulitic primary phase. The magnesium-alloyed variant has a significantly smaller particle size of 35  $\mu\text{m}$  compared to that of the Al-Li-Cu alloy with 48  $\mu\text{m}$ . The form factor of the globulitic primary phase for both alloys is ~0.74. The “image-analyse” evaluation of the samples could detect no notable signs of mix separation across the step thickness. The solid phase proportion for the copper-alloyed type is ~75 % and for the magnesium-alloyed version ~65 % in both step thicknesses/cooling rates.

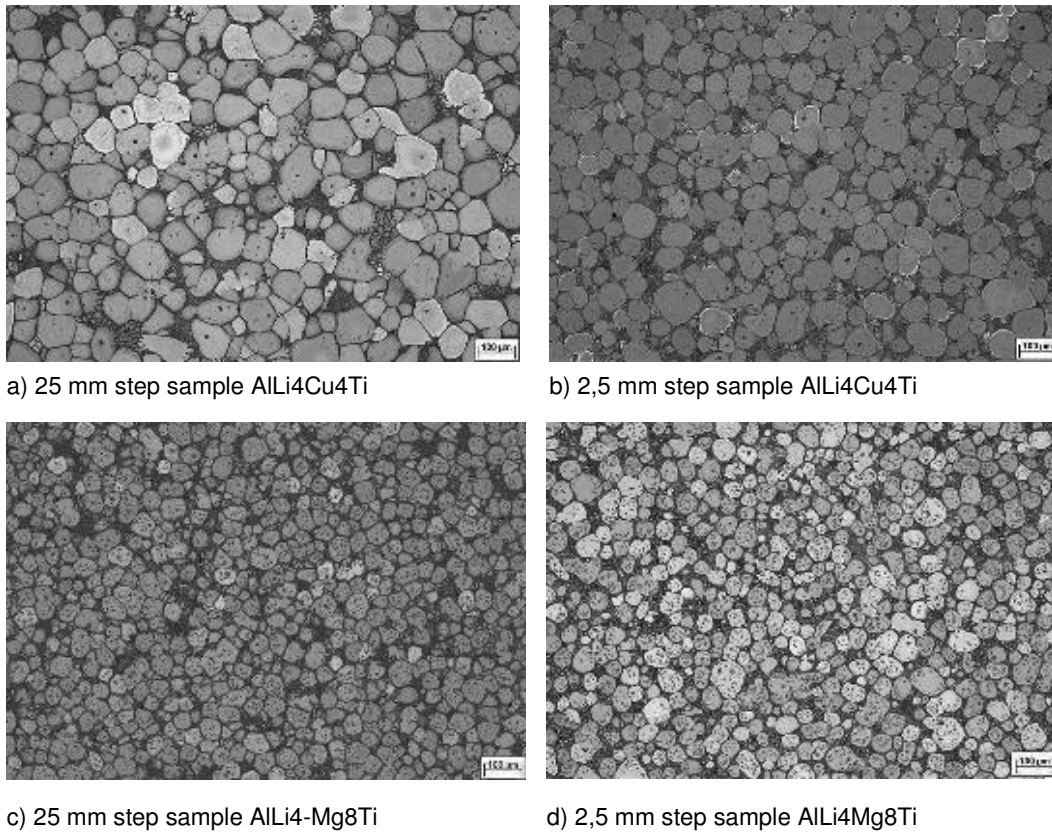


Figure 4.20: Microstructures of thixocast step samples (AlLi4Cu4Ti and AlLi4Mg8Ti) [33]

Selected thixocasting step samples of the two aluminium-lithium alloys underwent T6 heat treatment (AlLi4Mg8: 2 h at 430°C solution annealed, quenched in water, 15 h at 120°C precipitation heat treatment, AlLi4Cu4: 2 h at 510°C solution annealed, quenched in water, 15 h at 120°C precipitation heat treatment). Even after the heat treatment the globulitic grain structure was retained. In the case of the alloy AlLi4Cu4Ti several large globulites did indeed collect near the surface which, with 100 - 150 µm, had double the average grain size than that in the centre of the steps (50 - 80 µm). In contrast to this, the alloy AlLi4Mg8Ti displayed a uniform grain size distribution between the centre of the step and the step surface in all steps (Figure 4.21).

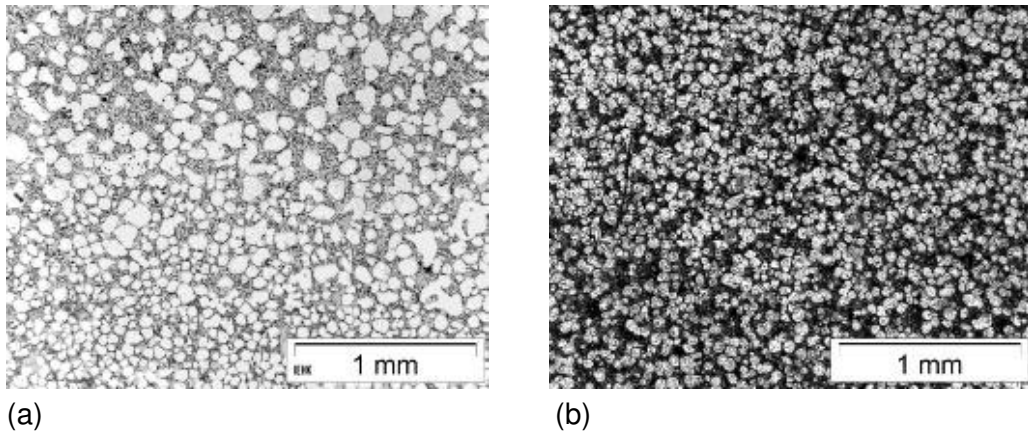


Figure 4.21: Phase separation near the surface of an Al-Li<sub>4</sub>Cu<sub>4</sub> (Al-Li<sub>4</sub>Cu<sub>4</sub>Ti) step sample (a) and near the surface of an AlLiMg<sub>8</sub> (AlLi<sub>4</sub>Mg<sub>8</sub>Ti) step sample (b)

#### 4.6.2 Rheocasting

On the basis of the experiences with thixocasting the 0.15 weight% Sc and 0.15 weight% Zr modified alloy AlLi<sub>2.1</sub>Mg<sub>5.5</sub> (A8) was selected, because due to the lower Li and Mg contents the embrittlement is reduced due to minimized intermetallic phase formation. Because firstly mechanical properties were to be determined, for the melt-based metallurgical raw material production refined aluminium (99.999%) and high-purity lithium (99.9 %) were used, so that the Na content would be kept as low as possible. Implementation of the RCP process for AlLi alloys required the modification of the process window, in particular that of the melt treatment. Due to the expected reactivity of the alloys the SiC melting crucible was closed in and flushed with argon gas. Refer to Section 4.4.2 for details of the process. Figure 4.22 shows the development of the micro structure commencing with the raw material and continuing through to forming by means of the Rheo-Container process. The billets synthesised by means of the overpressure melting process display a very fine granular structure of  $d_m \sim 40 \mu m$  average diameters. In the course of the RCP process the primary phase is formed with a more globular but also more coarse-grained aspect ( $d_m \sim 65 \mu m$ ).

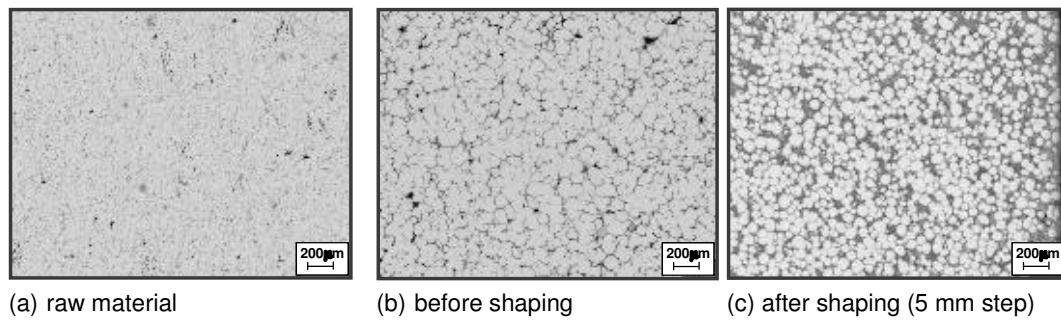


Figure 4.22: Development of the micro structure of  $\text{AlLi}_{2.1}\text{Mg}_{5.5}\text{ZrSc}$  in the course of the RCP [32]

The very homogenous distribution of the primary alpha-solid solution across all wall thicknesses in the step sample is shown in Figure 4.23.

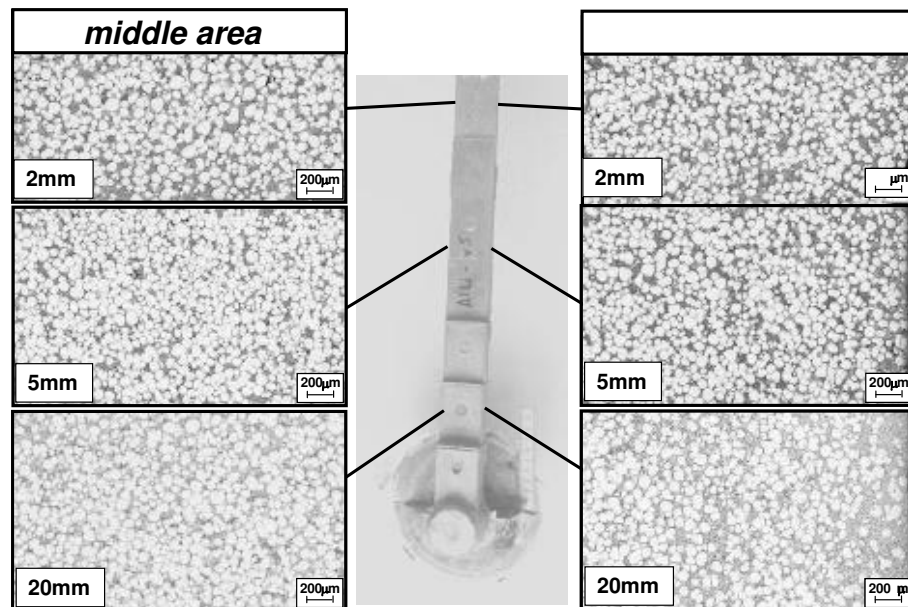


Figure 4.23: Microstructure of an  $\text{AlLi}_{2.1}\text{Mg}_{5.5}\text{ZrSc}$  alloy processed in partially liquid state (at  $T = 601^\circ\text{C}$ ) by means of the RCP [32]

The average grain size of the  $\text{AlLi}_{2.1}\text{Mg}_{5.5}\text{ZrSc}$  alloy was determined at  $65 \mu\text{m}$  as mentioned above. A significant tendency to mix-separation of the solid and liquid phase was not observed. Only in the immediate border area of the component the liquid phase did become concentrated. In statistically distributed samples for determining the alloy composition there were indications that the target composition could largely not be set in relation to the main alloying elements of Li and Mg (Figure 4.24). This is on the one hand due to the already demonstrated non-homogeneity in the raw material or to burning off of the alloying elements during the forming process. Insofar this was to be improved for the extensive forming of real components.

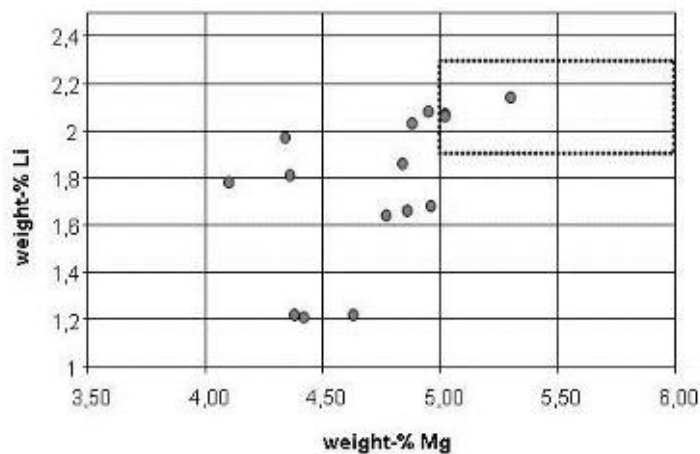


Figure 4.24: Li- and Mg-contents of the Al-Li-X step samples (specification for A1420 see rectangle)

The modification in the micro structure during heat treatment is shown in Figure 4.25. Two different T6 heat treatment strategies were tested. Already after a short solution annealing for a period of 3 hours, dissolving of the eutectic and intermetallic phase portions commences, enhancing the aluminium-mix crystal. This accompanied by slight grain growth. If the solution annealing time is extended to 24 h then the modifications in the micro structure are drastic in contrast.

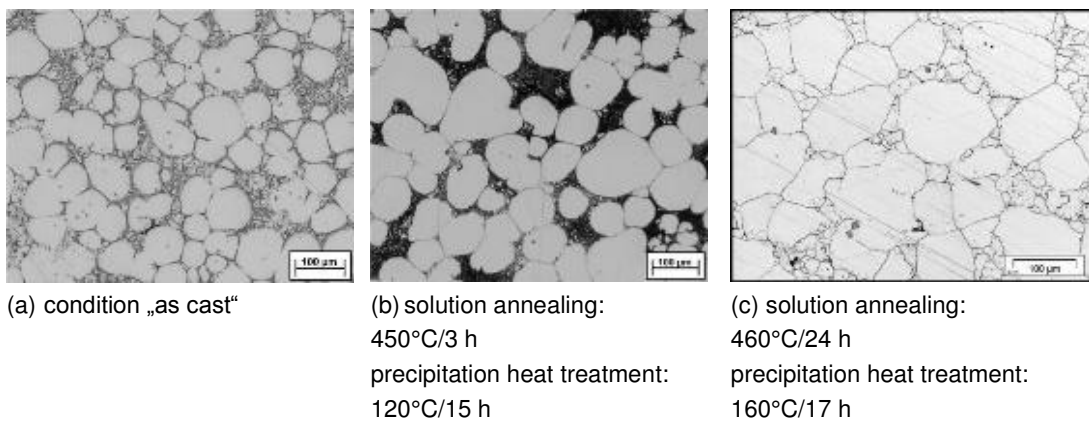


Figure 4.25: Microstructure of AlLi<sub>2.1</sub>Mg<sub>5.5</sub>ZrSc alloy processed by means of the RCP in its "as cast" state and after two T6 heat treatment states (5 mm step) [32]

Almost only the aluminium-mix crystal remains with a slight residual phase of Al<sub>2</sub>LiMg on the grain boundaries. In this state the micro structure resembles that of an aluminium moulding alloy. The addition of the elements Sc and Zr allowed

good grain refinement to be achieved and undesired grain growth as well as re-crystallisation to be successfully inhibited during the solution annealing.

The mechanical properties of various step samples were analysed in their "as cast" and T6 states. The "as cast" properties revealed no technically noteworthy results, neither for static strength nor for elongation values (Figure 4.26). After a 24 h solution annealing at 460°C, quenched in water and subsequently precipitation heat treatment at 160°C for 17 hours the average tensile strength was increased from 160 to above 380 MPa, the average yield limit from 100 to above 230 MPa and the average elongation from 2 to over 7 %. Some samples even achieved a tensile strength of 432 MPa, a yield limit of 250 MPa and an elongation of 13 %. The results in relation to the form-filling capacity displayed, as previously during the thixocasting tests, the excellent suitability of the Al-Li-x alloys developed. Only at the critical transformation from the 5 mm to the 2 mm step could some small (hot) cracking be identified on the component. For the subsequent real component production this effect should be avoided by choosing a lower processing temperature and therefore a higher solid/liquid ratio. An adapted tool geometry as well as locally adapted heating/cooling strategy can further reduce this tendency to hot tearing.

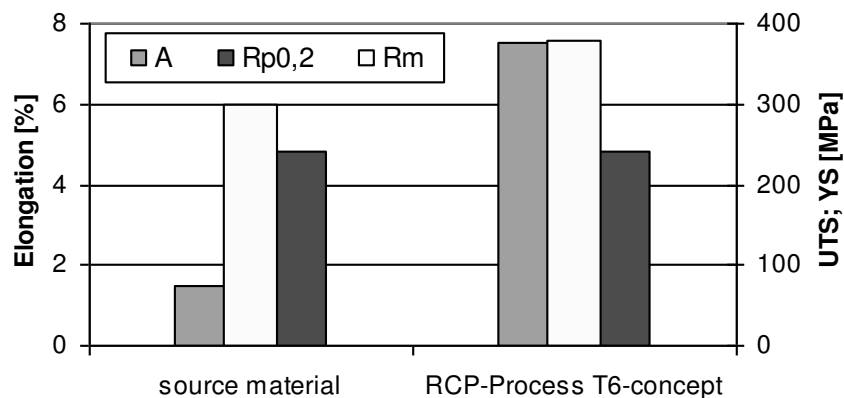


Figure 4.26: Mechanical properties of step samples made from Al-Li<sub>2.1</sub>Mg<sub>5.5</sub>Zr<sub>0.15</sub>Sc<sub>0.15</sub> (at cast and after annealing) [34]

#### 4.7 Production of Al-Li Demonstrators by Rheocasting

In order to check the transferability of the laboratory results under production conditions, a tie-rod was selected as a real component and was produced at the Foundry Institute of RWTH in Aachen using the Rheo-Container process on the basis of the Al-Li-X raw material billets [35]. This component has previously been proved using the alloy A356 [33]. The results of these works are given in more

detail in chapter 9. Using the overpressure melt process the Al-Li-X alloys were reproducibly produced in 3 kg scale with Li contents of 1.5 - 4 weight%. In order to prevent contamination by Na and K, it is necessary to employ pre-alloys and metals of high purity. The maximum Li losses compared to the initial weighing amounted to ~5 %. Using the permanent mould system available it was not yet possible however to prevent chemical non-homogeneity of the raw material billet. In particular the elements Cu and Mg are concentrated at the surface of the billet and are below the target values in the centre of the billet. DTA tests confirmed the results of the thermochemical prediction calculations that for the  $\text{AlLi}_4\text{Cu}_4$ ,  $\text{AlLi}_4\text{Mg}_8$  and  $\text{AlLi}_{2.1}\text{Mg}_{5.5}$  alloy systems the largest process window for processing in the semi-solid range can be expected. The evaluations for the microstructure in the semi-solid range for quenched samples indicate that in particular the Ti and Zr grain-refined alloys  $\text{AlLi}_4\text{Cu}_4$  and  $\text{AlLi}_4\text{Mg}_8$  as well as the Sc and Zr micro-alloyed alloys  $\text{AlLi}_{2.1}\text{Mg}_{5.5}$  achieve very good results with globular and fine grained grain structures in the range of 38 - 60  $\mu\text{m}$ . Apart from that, these alloys have a high proportion of pre-melting eutectic phase, which supports thixotropic flow during forming.

The alloys  $\text{AlLi}_4\text{Cu}_4\text{Ti}$  and  $\text{AlLi}_4\text{Mg}_8\text{Ti}$  with billet formats of 160 mm x 75 mm were able to be transformed into the semi-solid state by inductive reheating without any problems. Excessive oxidation of the surface of the billet could be minimised by wrapping it with aluminium foil. The primary grain sizes achieved in the thixocast step samples were ~65  $\mu\text{m}$ , whereby this was very globular and homogeneously distributed over all step thicknesses. The thixotropic flow characteristics can in this respect be described as "excellent". The Sc and Zr micro-alloyed A1420 ( $\text{AlLi}_{2.1}\text{Mg}_{5.5}$ ) alloys were successfully processed using the Rheo-Container process at the Foundry Institute. Also in this case grain sizes of ~60  $\mu\text{m}$  were achieved in the "as cast" state. As indicated by the chemical analyses, with the RCP process a slight Li burn-off is to be taken into account due to the nature of the process. No tendency to mix-separation of the solid/liquid phase was identified. Only in the immediate shell the liquid phase was concentrated. After suitable heat treatment (solution annealed at 450°C for 24 h, quenched in water, precipitation heat treated at 160°C for 17 h) and the virtually full dissolving of the residual intermetallic phases, in the principle component (step sample) made from the alloy A1420 ( $\text{AlLi}_{2.1}\text{Mg}_{5.5}+\text{ScZr}$ ) mechanical characteristic values were achieved that are within the range of rolled sheets and profiles of the same alloy, and in the case of elongation even exceed them. Due to the high-purity raw material used here, it was possible to safeguard the mechanical properties by keeping the Na content below 6 ppm. In direct comparison to the rolled alloy 1421 (Sc added) it appears that for a semi-solid

cast component, already in this early step of development, ~80 % of the yield limit, 88 % of the tensile strength and equivalent elongations can be achieved. The anisotropy of mechanical properties occurring in rolled sheets does not occur in SSM-Al-Li components due to the homogenous microstructure achieved. By semi-solid forming of the reactive Al-Li alloys, that are difficult to process in conventional casting processes, a completely new production method and an innovative component quality for near-net-shape production is being achieved.

#### **4.8 Recycling of Aluminium-Lithium Alloys from Thixoforming Processes**

##### **4.8.1 State of the Art**

Since the commercial introduction of Al-Li moulding alloys in the late 1980s, the question of recycling has represented a challenge in many aspects [42]:

- The lithium contained in Al-Li residues represents a value far in excess of the aluminium content.
- The residues can cause problems if they enter the usual recycling route, especially in the foil sector.
- To date, the specifications for secondary casting alloys do not indicate any lithium content and an agglomeration of Al-Li residues is not without consequences, because in moist conditions it can react with the hydrogen being released.

In order to secure wider use of this group of alloys a complete recycling concept must be developed for the residues that would facilitate 100 % reuse of the recycled Al-Li residues. For recycling, firstly as much as possible a closed system ("closed-loop recycling") is desirable, in which the residues can be returned direct to the existing process and not need to be diverted through the entire secondary cycle for aluminium. In the case of scrap recycling this would probably not be feasible, because of the problems involved sorting of separated types of scrap the lithium would be lost.

In principle there are two possibilities for recycling of the thixo-materials. The first and by far the most sustainable solution would be to retain the valuable alloying elements within the alloy. This is primarily of interest in the case of clean scrap materials that could be melted down in molten salt. The second alternative would be to transfer the alloying elements (Mg, Li) into molten salt in order to subsequently reclaim them from there if required. Such a procedure could be



applied for clean as well as low-quality scrap materials. From the point of view of economy, the same molten salt should be used as that used in the secondary aluminium industry (70 % NaCl + 30 % KCl with 2 – 3 % CaF<sub>2</sub> additive), in contrast to the very hygroscopic mixture of LiCl and KCl proposed in [43] and [44]. Then recycling of the salt-slag produced could be performed in a largely conventional manner.

#### **4.8.2 Thermochemical Metal-Salt Equilibria**

In order to state which salt mixture compositions come into consideration for the two above-mentioned recycling alternatives, thermochemical calculations were performed in respect of the equilibria between the relevant alloys and various molten salts, using the FACTSAGE® program. Four alloy types were combined with salt mixtures, on the one hand based on NaCl and KCl with added CaF<sub>2</sub>, MgCl<sub>2</sub>, LiF, and on the other hand based on KCl and LiCl.

In the equilibria with KCl/NaCl/LiCl molten salts the calculations indicate for AlLi<sub>2</sub>Mg<sub>5.5</sub> that the Mg and Li contents of the metal melt would remain unchanged, but the Na and K contents, with a LiCl content of up to 50 %, would rise substantially but would rather fall steeply with a further increase in the LiCl content of the salt mixture.

For a proportion of just 10 % LiCl in the salt mixture the rise in the process temperature would lead to higher K contents in the metal melt, when the Na content remains unchanged. An increase in the LiCl content from 10 to 90 % in the salt mixture would reduce the Na and K contents in the metal melt by that factor. All calculations indicate that by melting an AlLi alloy using NaCl/KCl/LiCl salts generally no recyclable AlLi alloys can be reclaimed, because the Na and K contents would become unacceptably high. When using binary KCl/LiCl molten salts the calculated K content of the metal melt at 650°C, with 90 % LiCl in the molten salts, would reach a far lower value (Figure 4.27).

The degree of Li and Mg reclamation amounts to ~98 - 99.5 % (Figure 4.28), whereby the acceptable K content in the alloy is only reached if the LiCl content of the salt mixture is well above 90%.

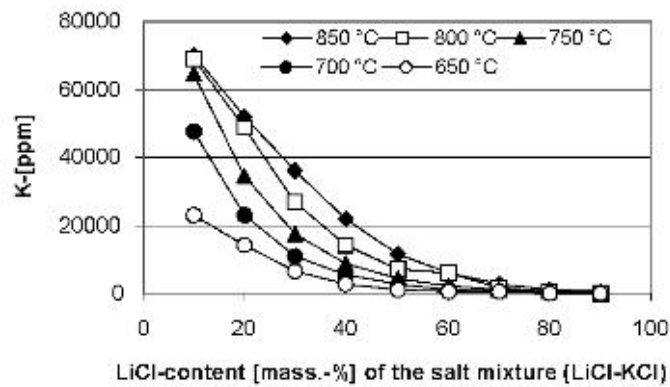


Figure 4.27: Calculated K contents equilibria of  $\text{AlLi}_2\text{Mg}_{5.5}$  after melting under molten  $\text{KCl/LiCl}$  (metal/salt ratio 1/1)

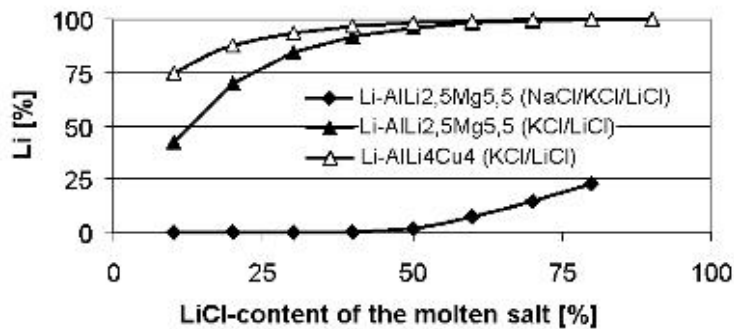


Figure 4.28: Calculated Li yield of Al-Li alloys at  $750^\circ\text{C}$  after contact  $\text{NaCl/KCl/LiCl}$  in dependence of the LiCl content of the salt mixture

#### 4.8.3 Experimental Validation of the Thermochemical Calculations

In order to minimise any possible diffusion inhibitions arising in the equilibrium set-up, intensive agitation was also provided for. Each salt mixture was melted in a firebrick/graphite crucible (diameter 80 mm, height 100 mm) and brought up to attempt temperature. The agitator was rotated ( $400 \text{ min}^{-1}$ ) and swarf of the applicable alloy was added. After melting and in further steps of 1, 3, 6, 10, 20, 30, 40, 50 and 60 min, salt samples were taken for ICP (Inductive Coupled Plasma) analysis and metal samples were taken before and after the attempt.

As an example for series 1 - 4, Figure 4.29 shows that during treatment of an  $\text{AlLi}_{2.5}\text{Mg}_4$  metal melt using  $70\text{NaCl}/20\text{KCl}/10\text{MgCl}_2$  molten salts, Li was fully transformed by  $\text{MgCl}_2$  into  $\text{LiCl}$  (Section 4.7.2). The equilibrium is attained in this case after a short period of 3 – 4 min. Also for the treatment of  $\text{AlLi}_4\text{Mg}_8$  alloy using  $70\text{NaCl}/27\text{KCl}/3\text{LiF}$  molten salts, the Li is fully transformed by the  $\text{NaCl}$  into  $\text{LiCl}$  and a small amount of Mg by  $\text{LiF}$  into  $\text{MgF}_2$ . The experimental testing in its entirety largely confirms the thermochemical calculations. The use of a  $\text{NaCl}/\text{KCl}$  salt mixture with additives of  $\text{LiF}$ ,  $\text{CaF}_2$  or  $\text{MgCl}_2$  leads to transfer of the Li from the metal alloy into the molten salts. When using  $\text{MgCl}_2$  as an additive the Mg content rises in correspondence with the transfer of Li into the molten salts, which could partially be compensated by the addition of  $\text{LiF}$ . By the addition of  $\text{CaF}_2$  a transformation of Mg into the molten salts is achieved, as well as that of the Li. As calculated in Section 4.7.2, the lithium is nearly completely transferred to the molten salts (residual content in the metal melt  $<0.1\%$ ) so that  $\text{AlLi}$  alloys can not be recycled using this salt mixture.

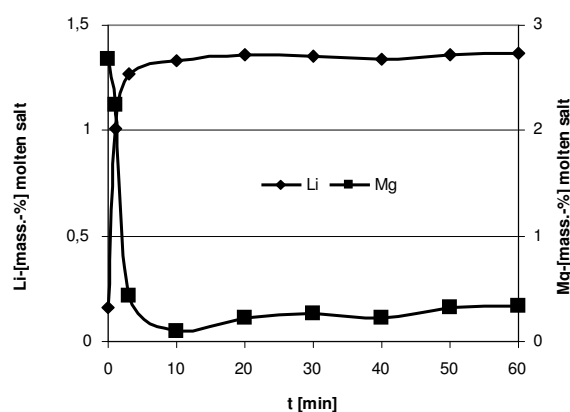


Figure 4.29: Kinetics of equilibrium tests for interaction of  $\text{AlLi}_{2.5}\text{Mg}_4$  with  $70\text{NaCl}+20\text{KCl}+10\text{MgCl}_2$  molten salt at  $750^\circ\text{C}$

The tests using a salt mixture of  $\text{KCl}$  and  $\text{LiCl}$  for melting residues from  $\text{AlLiMg}$  and  $\text{AlLiCu}$  did however indicate that it is possible to retain the Li and/or Mg completely in the metal melt, providing a  $\text{LiCl}$  content of more than 90 % in a  $\text{KCl}/\text{LiCl}$  salt mixture. In this case the experimental values for the K content in the metal are even lower than those forecast by the thermochemical calculations (Figure 4.30). In the course of the treatment of the  $\text{AlLiMg}$  metal melt with pure  $\text{LiCl}$  a K content of 14 ppm in the metal melt was achieved, with a Li and Mg yield of over 99.4 % in both cases. The reason for the lower experimental K contents in contrast to the theoretical values is that the solubility of K in solid and liquid aluminium was not available.

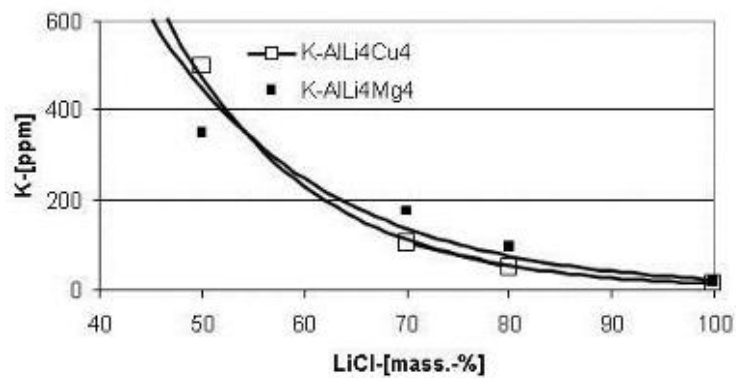


Figure 4.30: Experimental K contents in the metal after treatment of AlLi4Mg4 and AlLi4Cu4 melts using salt mixtures of KCl/LiCl at 750°C

In order to close the loop in the recycling of AlLi residues from thixoforming it would be necessary to process the produced salt slag. When using pure water-soluble LiCl for recycling, it is possible to treat the produced salt slag by means of the conventional dissolution-crystallisation process that is standard within the secondary aluminium industry. This closed loop for the recycling of Al-Li residues (Figure 4.31) enable a nearly complete recovery of reusable AlLi alloys as well as returning the used LiCl back into the recycling process.

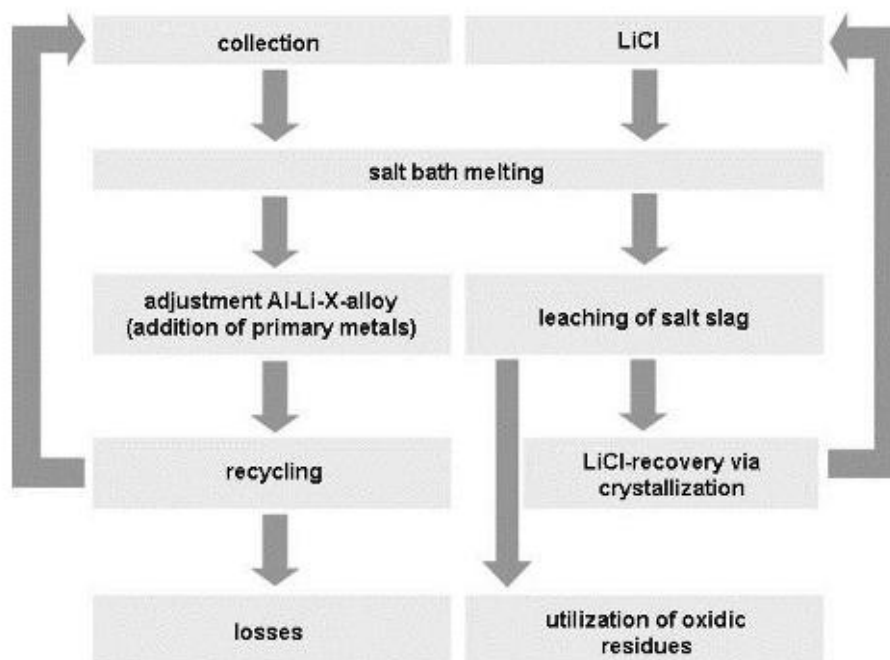


Figure 4.31: Almost closed-loop recycling of AlLi residues

## References

- [1] Fehlbier, M.: „Verarbeitung teilflüssiger metallischer Werkstoffe“, Dissertation RWTH Aachen 2002, ISBN 3-8322-1064-4, S. 9
- [2] Wagener W., Hartmann D.: „Feedstock material for semi-solid casting of magnesium“, Proceedings of the 6th International Conference of Semi-Solid Processing of Alloys and Composites, Turin, Sept. 2000, S. 301-306
- [3] Flemings M.C.: „Behavior of metal alloys in the semisolid state“, The 1990 Edward Campell Memorial Lecture, Metallurgical Transactions A, Vol. 22A, 1991, S. 957-980
- [4] Müller-Späth H.: „Legierungsentwicklung unter Einsatz des SSP-Verfahrens und Umsetzung intelligenter Materialkonzepte beim Thixogießen“, Dissertation RWTH Aachen, Gießerei-Institut: Forschung, Entwicklung, Ergebnisse, Shaker Verlag, Band 7, 1999
- [5] Wan G., Witulski R.: „Thixoforming of aluminium alloys using modified chemical grain refinement for billet production“, International Conference on Aluminium alloys: New process technologies, 3th-4th June 1993, Marina di Ravenna, Italy
- [5] Brusethaug S., Voje J.: „Manufacturing of feedstock for semi-solid processing by chemical grain refinement“, Proceedings of the 6th International Conference of Semi-Solid Processing of Alloys and Composites, Turin, September 2000, S. 451-456
- [6] Noll, T.: „Die anwendungsgerechte Weiterentwicklung des Al-Werkstoffes EN AC- $\text{AlSi7Mg0,3}$  (A356) mit chemischer Kornfeinung“, Dissertation RWTH Aachen 2003, ISBN 3-8322-2003-8
- [7] Hirt G., Sahm P.R.: „Möglichkeiten zur Produktivitätssteigerung, Qualitätsverbesserung und Materialeinsparung durch endabmessungsnahe Fertigung mit kombinierten Ur-/Umformverfahren“, EFU-Mitteilungen 1-1994
- [8] Loue W.R.: „Metallurgische Aspekte des Thixogießens der Aluminiumlegierungen  $\text{AlSi7W1gO,3}$  und  $\text{AlSi7MgO,6}$ “, Gießerei-Praxis, Nr. 13/14, 1996, S.251-260
- [9] Decker R.: „Casting semi-solids by Thixomolding“, Foundry Focus Autumn/Winter 1990, S. 22-23
- [10] Decker R., Carnahan R. D.: „Thixomolding“, Advanced Materials Technology 1991, 8. 174-179
- [11] Dworog A. et al.: „Formfüllvorgänge beim Magnesiumspritzgießen“, 8. Magnesium Abnehmer Seminar, Aalen, 14./15. Juni 2000
- [12] Decker R. F., Carnahan R. D.: „Thixomolding“, Thixomat Inc., Ann Arbor, Michigan, USA, 47\* Mg-Conference, 1991, S. 106-116

- [13] Gullo, G. C. „Thixotrope Formgebung von Leichtmetallen – neue Legierungen und Konzepte“, Dissertation ETH Zürich, 2001, Diss.ETH Nr. 14154
- [14] Prikhodovsky, S.: Modellierung von Reifungsprozessen und Anwendung auf das Thixoforming, Deutsche Dissertation: (2000), ISBN: 3-826-7618-7
- [15] Steinhoff, K.; Gullo, G. C.; Kopp, R.; Uggowitzer, P. J.: A new integrated Production Concept for Semi-Solid Processing of high Quality Al-Products, Proc. 6th Int. Conf. Semi-Solid Processing of Alloys and Composites, Turin, Italy, 27-29 Sept. 2000, Publ. Edimet Spa, Brescia, Italy, Seite 121-127
- [16] Harris, S. J.; Noble, B.; Dinsdale, K.: in: T.H. Sanders Jr., E.A. Starke Jr. (Eds), Proc. 2nd Int. Conf. on Aluminium-Lithium alloys II, TMS, Warrendale, PA (1983) 219.
- [17] Kammer, C.: Aluminium-Taschenbuch, B. 1, Grundlagen und Werkstoffe, 15 Auflage, S. 303, Aluminium-Verlag, Düsseldorf, 1995
- [18] R. Davis, J. R.: in: Davis and Associates (Eds.), ASM Specialty Handbook, Aluminum and Lithium alloys, Ohio, ASM International (1998).
- [19] Starke, E. A.; Sanders Jr.: in: Engineering Materials Advisory Services (Ed.), Proc. 1st Int. Conf. on Aluminum alloys: Their Physical and Mechanical Properties; England (1986).
- [20] Bick, M.; Markwoth M.: Thoughts on the Removal of Lithium from Primary Aluminium and Experiments to Carry out the Process on a technical scale Metall 34 (1980) 12, Seite 1095-1098
- [21] Bofarini, C.: „Prozessentwicklung des Feingießens von AL-Li Legierungen sowie Untersuchungen ihrer gießtechnischen und mechanischen Eigenschaften“, Gießereiforschung 43, 1991, Nr.2
- [22] Polmear, I. J.: Light Alloys-Metallurgy of the light metals, A member of the Hodder Headline Group, London-New York-Sydney-Auckland, 1989, p. 130-132
- [23] Vekateswara R.; Yu, W.; Ritchie, R. B.: Metal. Trans. A 19 (1988) S. 563.
- [24] Miller, W. S.; White, J.; Eloyd, D. J.: in: G. Champier, B. Dubost, D. Miannay, E. Sabetay (Eds.), Proc. 4th Int. Conf. on Aluminium-Lithium alloys IV, Paris, J. de Phys Colloque, 48 (1987) C3: 139.
- [25] Webster, D.: „Aluminium-Lithium alloys, the next generation“, Adv. Materials & Processes, Band 145 (1994), Heft 5, Seite 18-24
- [26] Sweet, E. D. et. al., Proceedings 4th International Conf. on Al-Alloys, Georgia Institute of Technology, Atlanta, USA, p.231, 1994
- [27] Kopp, R. et. al.: Sonderforschungsbereich SFB 289: Formgebung metallischer Werkstoffe im teilerstarrten Zustand und deren Eigenschaften, Arbeits- und Ergebnisbericht 2002/2003/2004 für die Deutsche Forschungsgemeinschaft DFG, S. 54-56

- [28] Balitchev, E., „Thermochemische und kinetische Modellierung zur Legierungsauswahl mehrphasiger Systeme für das Thixoforming und zur Optimierung ihrer Formgebungsprozesse“, Dissertation, RWTH Aachen, 2004
- [29] Balitchev, E.; Hallstedt, B.; Neuschütz, D.: „Thermodynamic Criteria for the Selection of Alloys Suitable for Semi-Solid Processing“, *steel research int.* 76 (2005) No 2/3, p. 92-98
- [30] Fridlyander, I.N.; Rokhlin, L.L.; Dobatkina, T.V.; Nikitina, N. I.: „Phase equilibria in aluminium alloys containing lithium“ (russisch), *Metallovedenie i Termicheskaya Obrabotka Metallov*, No. 10 (1993). S. 16-19
- [31] Hemminger, W.; Cammenga, H.: „Methoden der Thermischen Analyse“, Springer Verlag, 1989, ISBN: 3-540-15049-8
- [32] Höhne, G.; Hemminger, W.; Flammersheim, H.-J.: „Differential Scanning Calorimetry – An Introduction for Practitioners“, Springer Verlag, 1996, ISBN: 3-540-59012-9
- [33] Kopp et. al.: „Sonderforschungsbereich SFB 289: Formgebung metallischer Werkstoffe im teilerstarrten Zustand und deren Eigenschaften“, Arbeits- und Ergebnisbericht 2002/2003/2004 für die Deutsche Forschungsgemeinschaft DFG, Seite 165
- [34] Sauermann, R.; Friedrich, B.; Grimmig, T.; Bünck, M.; Bührig-Polaczek, A.: „Development of Al-Li alloys processed by the Rheo Container Process“, *Processings of the 9th International Conference on Semi-Solid Processing of Alloys and Composites*, 11-13.09.2006, Busan, Korea
- [35] Sauermann, R.; Friedrich, B.; Püttgen, W.; Bleck, W.; Balitchev, E.; Hallstedt, B.; Schneider, J. M.; Bramann, H.; Bührig-Polaczek, A.; Uggowitzer, P. J.: „Aluminium-Lithium Alloy Development for Thixoforming“ *Z. für Metallkunde* 95 (2004), 12, S. 1097-1107
- [36] Antrekowitsch, H.: „Grundlagenuntersuchungen bei der Erstarrung der Nichteisenmetalle Al und Cu im rotierenden Magnetfeld sowie Anwendungsmöglichkeiten in der Industrie“, Dissertation am Institut für Technologie und Hüttenkunde der Nichteisenmetalle an der Montanuniversität Leoben, 1998
- [37] Sommerhofer, H.; et.al. „Druckabhängigkeit des Gleichgewichts im System Al-Si“, *Gießereiforschung* 53 (2001) Nr.1, S. 25-29
- [38] Ohm, L.; Engler, S.: „Treibende Kraft der Oberflächenseigerungen beim NE-Strangguss“, *Metall* 43 (1989) S. 520-524
- [39] Buxmann, K.: „Mechanismen der Oberflächenseigerung von Strangguss“, *Metall* 31 (1977) S. 163-170
- [40] Cernov, D. B.; Schinyaev, A.: „Influence of High Pressure on the Composition Diagram of the Al-Si-System“, *Volume Struktura FAZ*, Nauka (1974) S.80-84

- [41] Batischev, A. I.: "Kristallisation von Metallen und Legierungen unter Druck", Titel: Russisch, Verlag Metallurgie - Moskau, 1977
- [42] Krone, K.: „Aluminium Recycling - Vom Vorstoff bis zur fertigen Legierung“, Aluminium-Verlag Marketing und Kommunikation GmbH, Düsseldorf, 2000
- [43] Mulate, K.: „Recycling von Mg-Li-Legierungen: Gleichgewichte zwischen Metall- und Salzschnmelzen“, Dissertation, Technische Universität Claustahl, 2000
- [44] Schwerdfeger, K., Mulate, K., Ditze, A.: „Recycling of Magnesium Alloys: Chemical Equilibria between Magnesium-Lithium-Based Melts and Salt Melts“, Metallurgical and Materials Transactions, V. 33B, Jun. 2002, p. 335-364